# Techniques for thin films of complex compounds

10.06.2015, Ionela Vrejoiu

# MOLECULAR BEAM EPITAXY (MBE)

MBE involves the generation of fluxes of constituent matrix and doping species (molecular beam) and their reaction at the (hot) substrate to form an ordered overlayer (epitaxy).

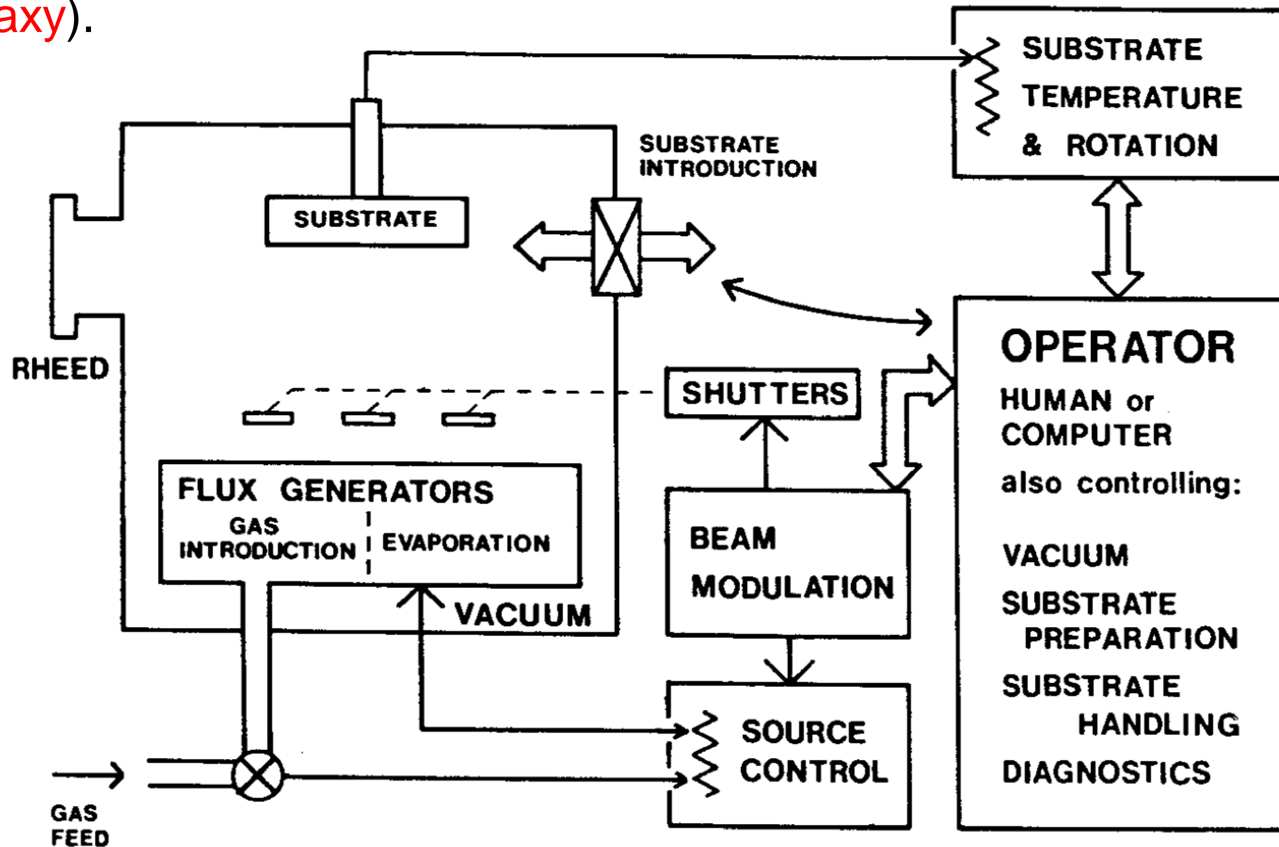


MOLECULAR BEAM
EPITAXY
Applications to Key Materials

Edited by
Robin F. C. Farrow
IBM Almaden Research Center
San Jose, California

np NOYES PUBLICATIONS
Park Ridge, New Jersey, U.S.A.

**Figure 1.** Schematic representation of the MBE process and control interface. The evaporation procedure, flux incidence on the substrate, vacuum, and process diagnostics are controlled by a supervisory operator or computer. The MBE process is supplemented by *ex situ* substrate preparation and wafer introduction procedures.

Elemental or compound constituents are heated (if in the liquid or solid state) or introduced (if gaseous) to cause mass transfer from the flux generators to the substrate, via the vapor phase.

To maintain the high purity and integrity of the deposit, stringent vacuum conditions are needed. MBE is essentially a line-of-sight technique from source to substrate, and the fluxes of constituents (and thus the composition of the material perpendicular to the growth direction) can be temporally modulated either by altering the evaporation/introduction conditions, or by physically interrupting the beam using rapid action mechanical shutters.

A key attribute of MBE is the precision with which the composition and doping of a structure can be tailored, such that atomically abrupt features can be produced. To achieve this level of control within realistic time spans, deposition rates centered around one atomic layer (a monolayer) per second are used. This places constraints on the operational temperatures of sources, and the speeds with which shutters are required to operate.

# Example: MBE for fabricating GaAs and doped GaAs films

One of the recent advances in MBE technology incorporates a gas source to supply As and P, as shown in Fig. 7-21b. Organometallics used for this purpose are thermally cracked, releasing the group V element as a molecular beam into the system. Excellent epitaxial film quality has been obtained by this hybrid MBE–OMVPE process, which is known by the acronym MOMBE. Hydride gas sources (e.g., $AsH_3$, $PH_3$) have also been similarly employed in MBE systems.

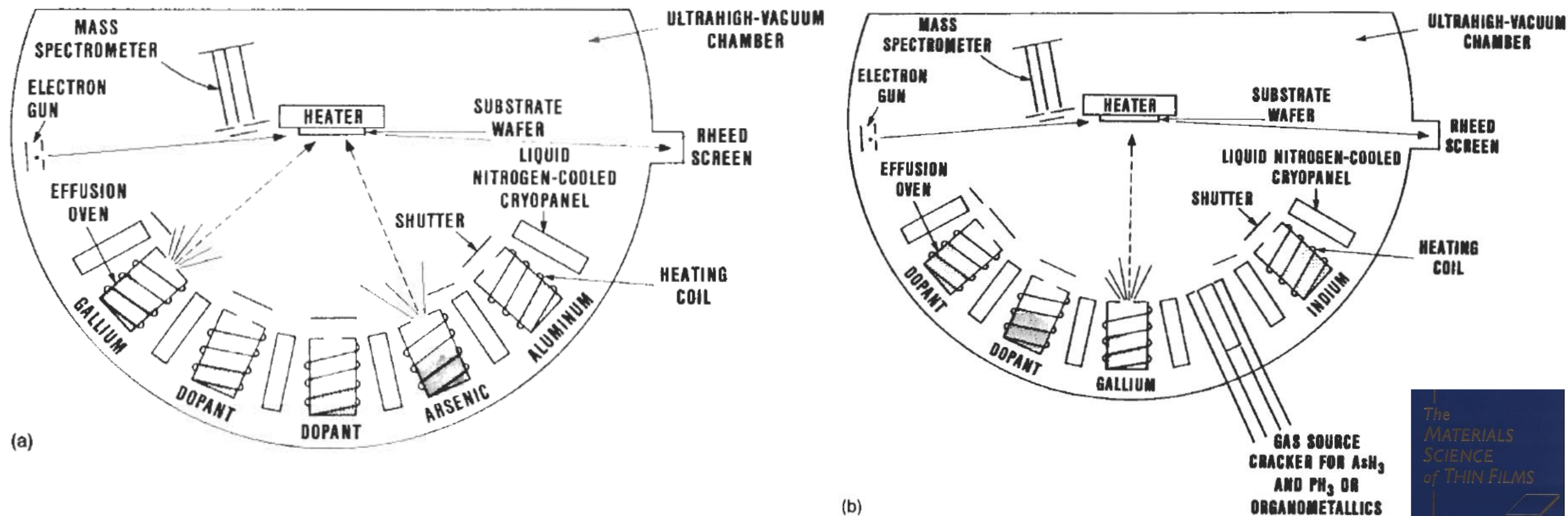


**Figure 7-21.** Arrangement of sources and substrate in (a) conventional MBE system, (b) MOMBE system. (Courtesy of M. B. Panish, AT&T Bell Laboratories.)

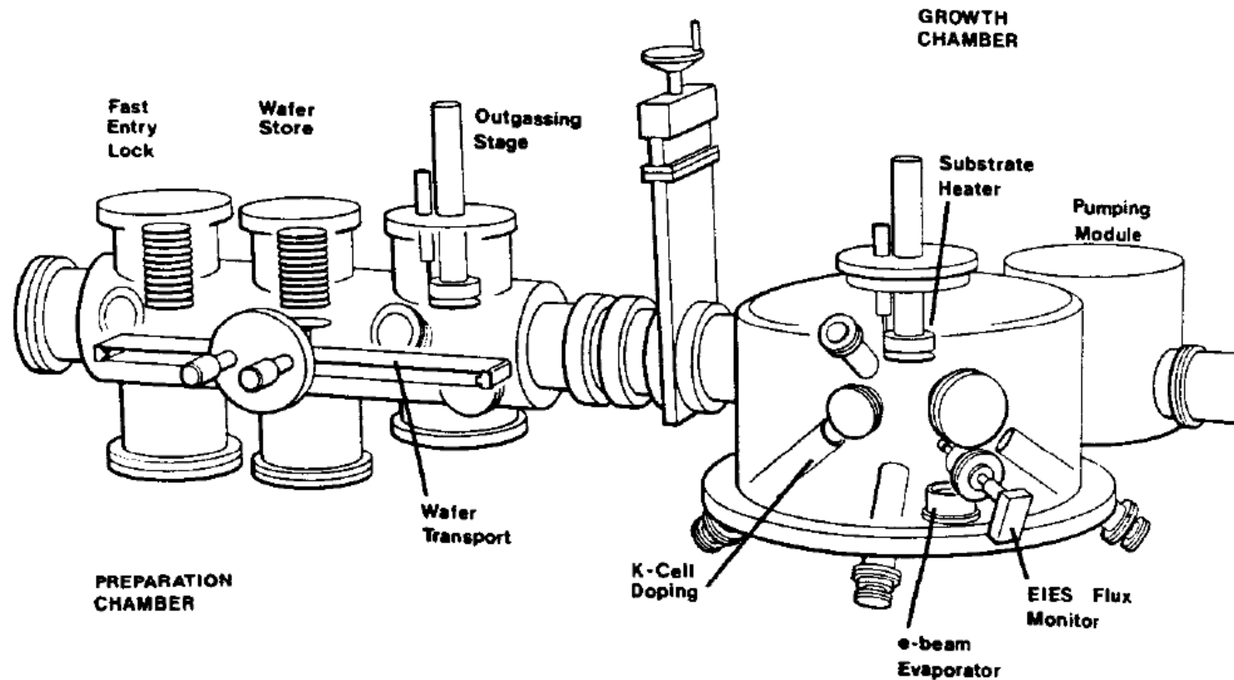


**Figure 3.** Schematic of an MBE system used for deposition of Si and related materials, metals, and superlattices. The matrix evaporation sources are electron beam evaporators (Sec. 5.4), although thermal effusion (Sec. 5.1), ion beam (Sec. 5.7) and other species specific (Sec. 5.1) sources can be fitted for matrix and doping flux generation. The deposition geometry is configured to achieve optimal uniformity of deposit (see Sec. 12). Shutters (Sec. 6) can interrupt the flux to yield rapid changes in composition or doping. The deposition chamber is connected via an in-line gate valve to the preparation chamber, in which substrate storage and diagnostics can be performed, and to a fast entry chamber (Secs. 2 and 3). Ultra high vacuum conditions are maintained throughout the system to achieve high material quality (see Sec. 3). The MBE system shown handles wafers up to 150 mm diameter without the need for wafer holders. *(Courtesy VG Semicon.)*

MOLECULAR BEAM EPITAXY
Applications to Key Materials

Edited by
Robin F. C. Farrow
IBM Almaden Research Center
San Jose, California

np NOYES PUBLICATIONS
Park Ridge, New Jersey, U.S.A.

# MOLECULAR BEAM EPITAXY (MBE): importance of ultra-high vacuum (UHV conditions)

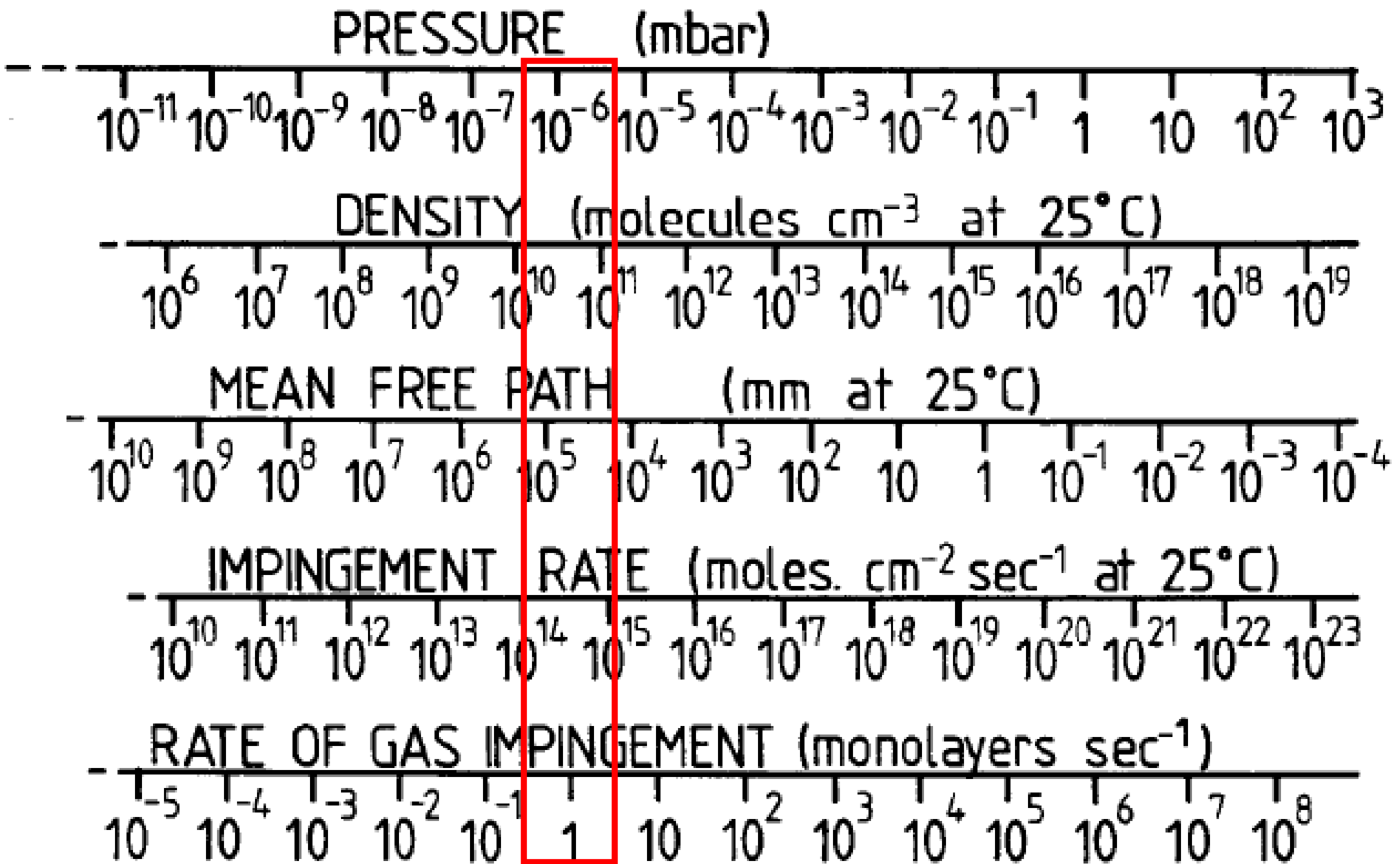


**Figure 4.** The relationship between the fundamental units encountered in vacuum technology.

# Schematic diagram of RHEED

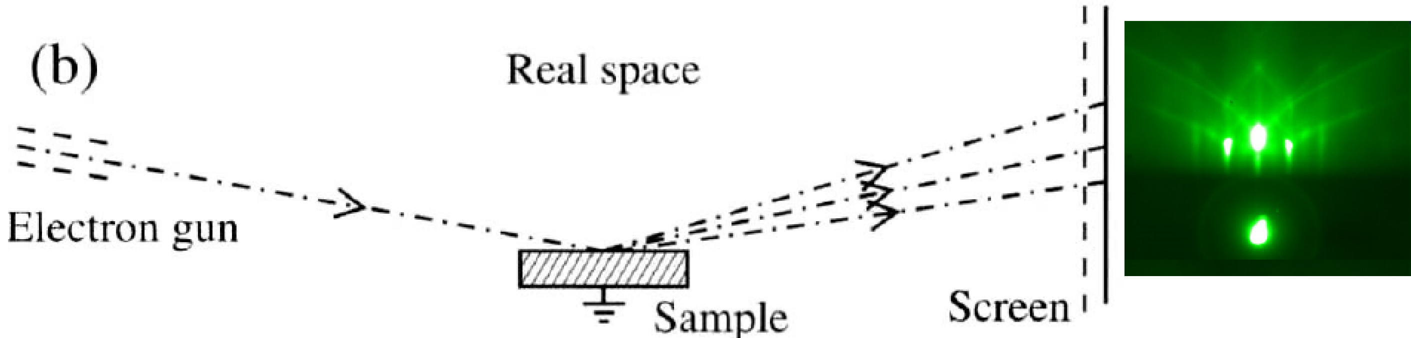


Wavelength of electron:

$$\lambda \approx 1.23 / \left[V\left(1+1.95\times10^{-6}V\right)\right]^{1/2} nm$$

| V(kV) | λ(Å) |
|---|---|
| 1 | 0.389 |
| 10 | 0.122 |
| 20 | 0.0853 |
| 25 | 0.0760 |
| 30 | 0.0690 |
| 50 | 0.0525 |

Energy of electron: 5 – 50 keV
Incident angle: < 5º

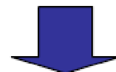

Geometrical feature in reciprocal space:

**Large** radius of the Ewald sphere with the **small** scattering angles

# Reflection high energy electron diffraction (RHEED)

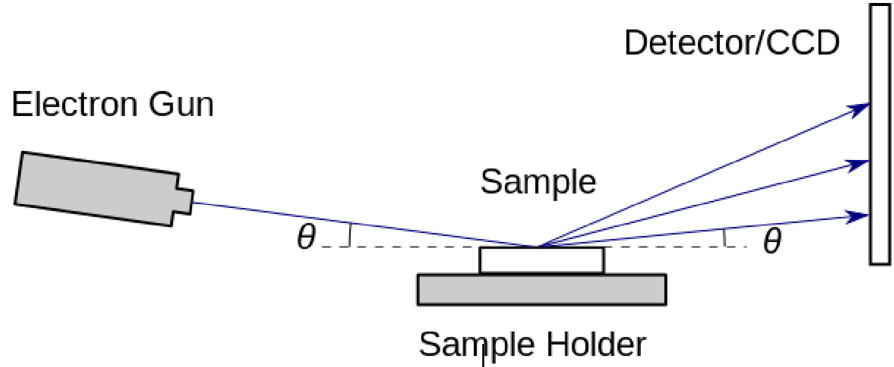


Reciprocal space for 2D lattice

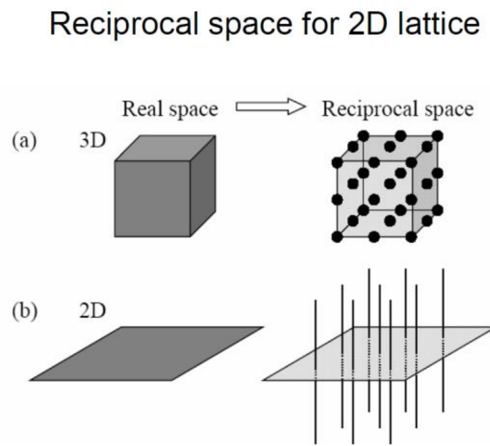


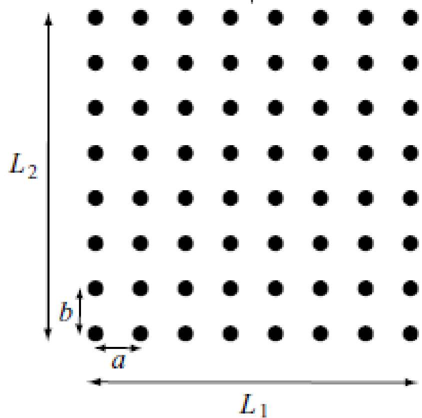


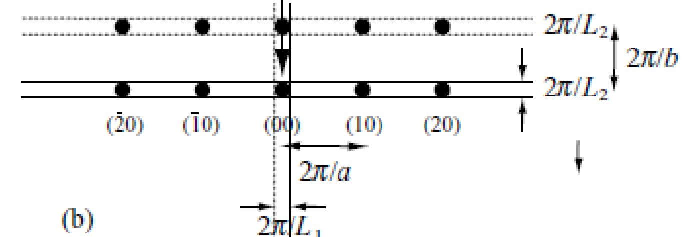


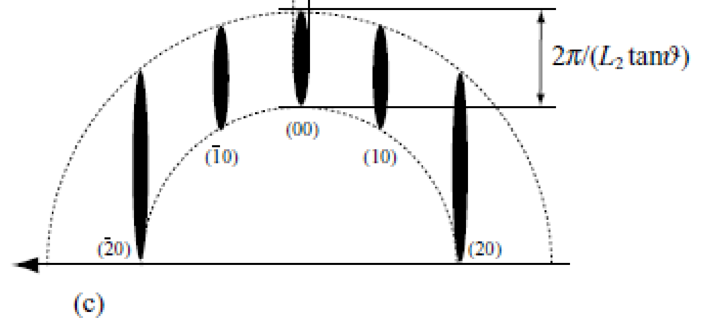


Figure 2.1 Explanation of the origin of RHEED streaks. (a) Arrangement of the two-dimensional array of lattice points. The finite sizes, $L_1$ and $L_2$, of the lattice are perpendicular and parallel to the incident direction, respectively. The incident direction is indicated by the arrow. (b) Reciprocal lattice for the arrangement in (a). (c) RHEED construction for (b); the lengths of the streaks depend on the glancing angle of incidence, $\vartheta$.

# Ewald Sphere for RHEED (ideal conditions)

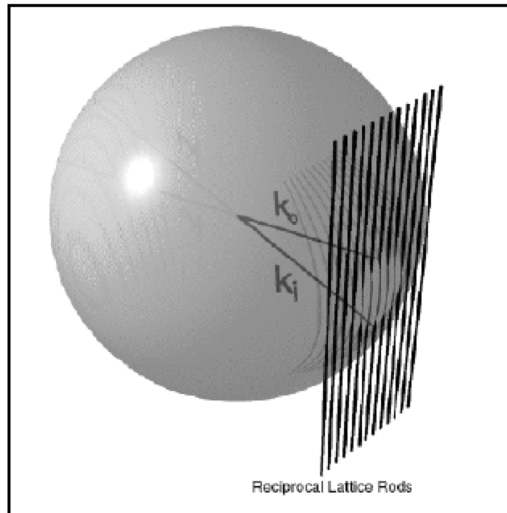


Ewald Sphere (infinitely thin)

Reciprocal Lattice Rods (infinitely thin)

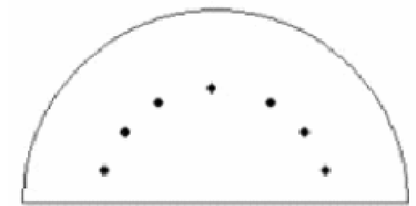

RHEED spots

Diffracted e-beams $k_f$

$\Delta k$

Incoming e-beam $k_i$ (Monochromatic)

sample (perfect flat)

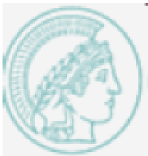

# Ewald Sphere for RHEED (real conditions)

*Sphere has thickness*: Electron beam diverges (not monochromatic)
*Rods have thickness*: Surface disorder (not perfect flat surface)

$\Delta\theta_f$

w

intersection

$\vec{K}_f$

$\vec{K}_i$

$1^{st}$ Zone

$0^{th}$ Zone

Sharp spots

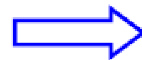

Elongated spots or Streaks

# RHEED in oxide research – diffraction pattern

Surface analysis during crystal growth

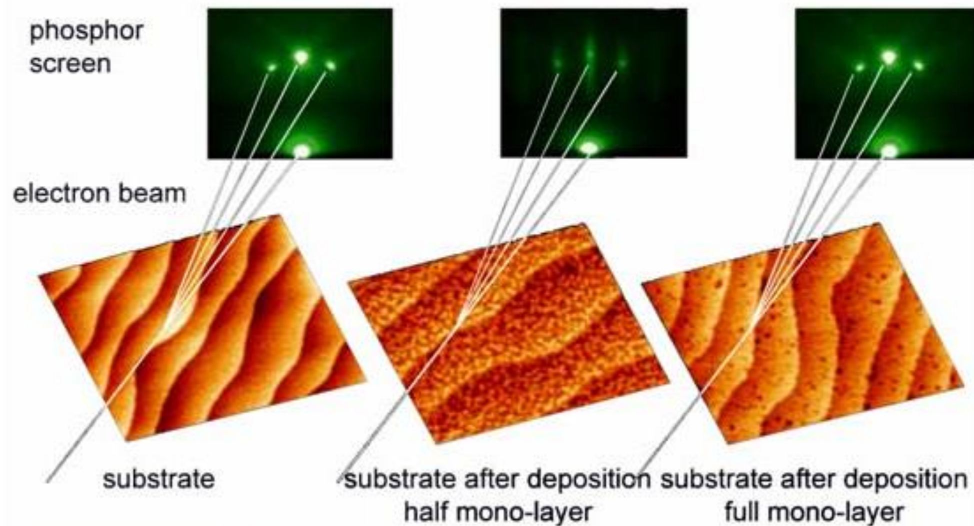


http://comp.uark.edu/

Analysis of surface reconstruction

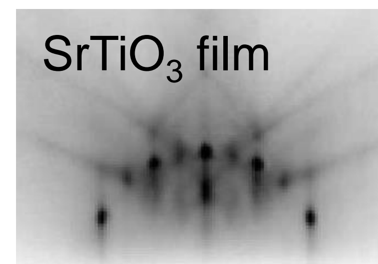


K. Iwaya *et al.*, APEX 3, 075701 (2010)

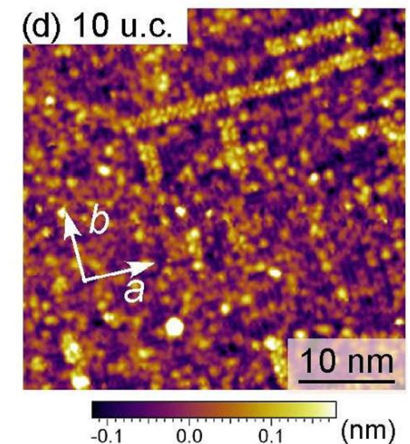


Takayuki Harada

# Reflection high energy electron diffraction (RHEED) for *in situ* monitoring of the growth

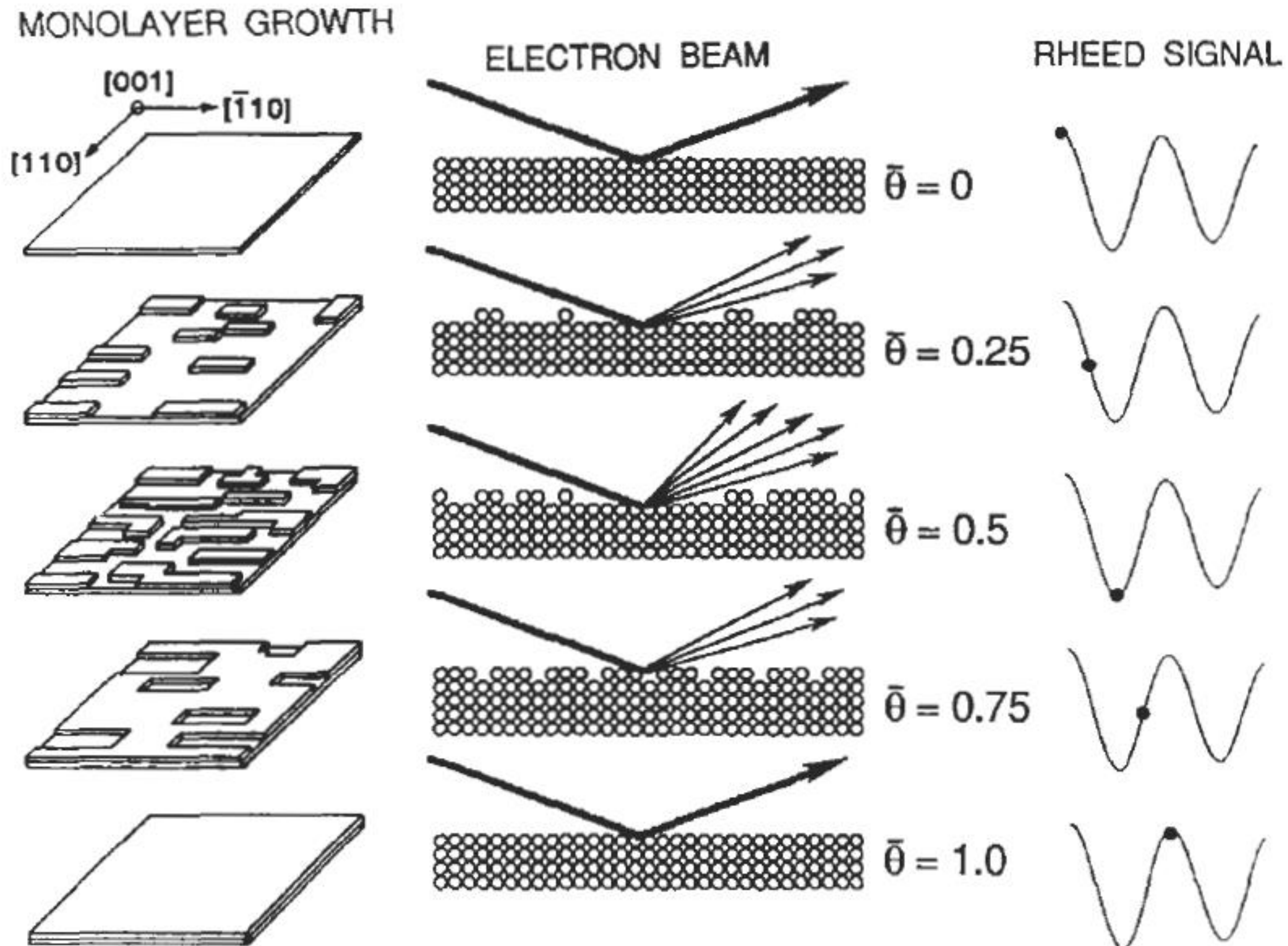


**Figure 7-22.** Real space representation of the formation of a single complete monolayer; $\bar{\theta}$ is the fractional layer coverage; corresponding RHEED oscillation signal is shown.

# RHEED Patterns: Morphology

**Perfectly flat surface**

a) Surface idéale

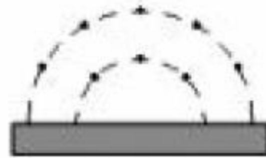

Sharp spots arranged on Laue rings

**Real flat surface**

b) Surface réelle

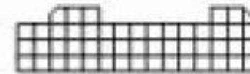

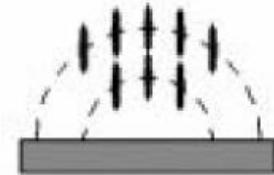

Streaks arranged on Laue rings

**Polycrystalline/Textured surface**

c) Polycristal

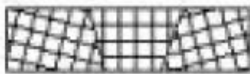

Polycrystalline: concentric rings
Textured: Concentric broken rings

**Rough surface**

d) Surface rugueuse

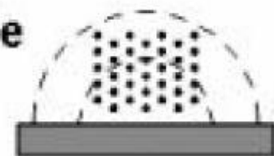

Spots in straight lines
(transmission pattern)

Thanks to Dr Wei Peng

# Reflection high energy electron diffraction (RHEED) for *in situ* monitoring of the growth

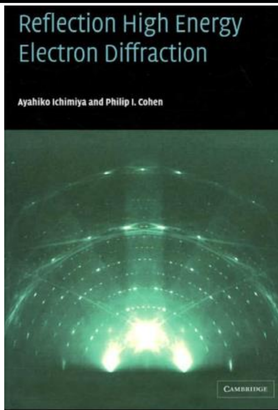


Layer-by-layer growth → Intensity oscillations

Intensity oscillation ⊗→ Layer-by-layer growth

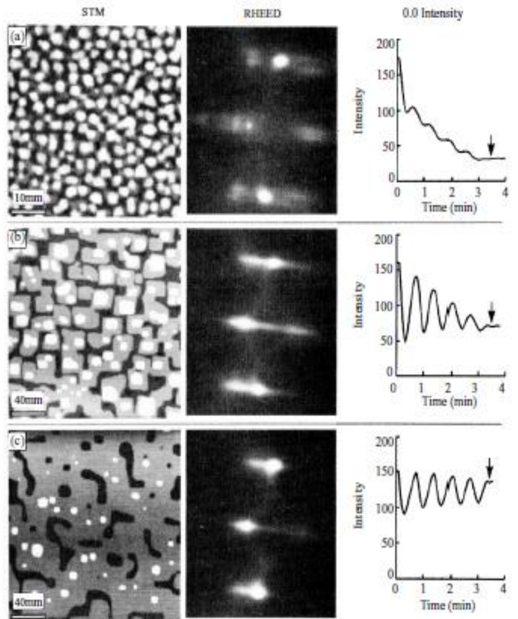


Figure 8.11 Combined real-space and reciprocal-space measurements of iron deposited on iron whiskers. Diffraction from islands is seen both in the patterns in the second column here and in the pattern in Fig. 8.10. In the top STM image the field of view is 500 Å while in the middle and bottom images it is 2000 Å.

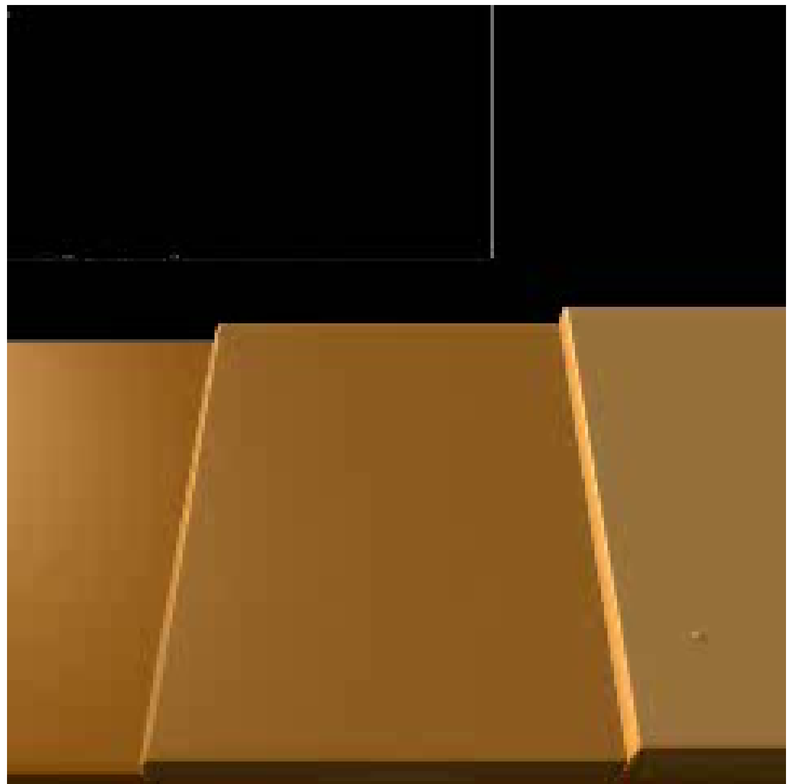

100 nm

# SPUTTERING: one result of interaction of energetic ions with surfaces

## Ion - Surface Interactions

Critical to the analysis and design of sputtering processes is an understanding of what happens when ions collide with surfaces. Some of the interactions that occur are shown schematically in Fig. 3-16. Each depends on the **type** of ion (mass, charge), the nature of surface atoms involved, and, importantly, on the ion energy. Several of these interactions have been capitalized upon in widely used thin-film processing, deposition, and characterization techniques:

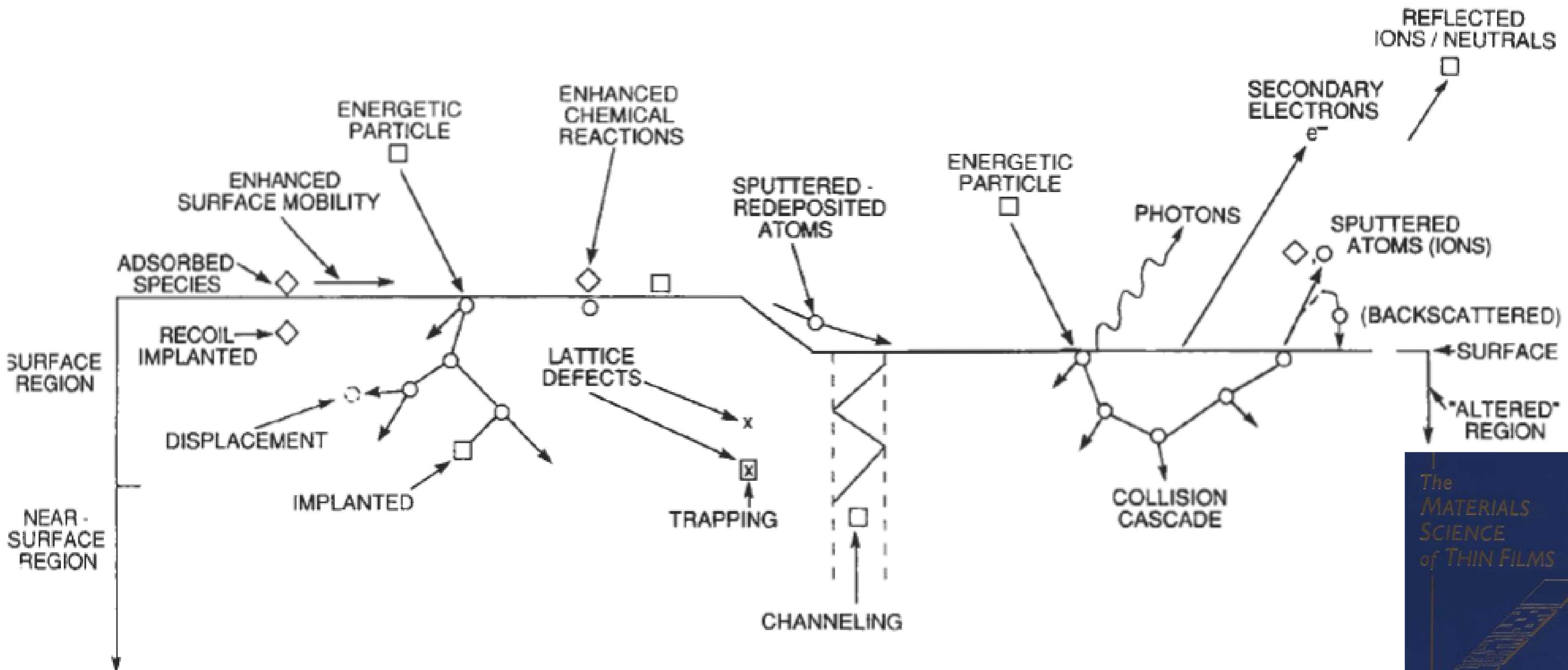


**Figure 3-16.** Depiction of energetic particle bombardment effects on surfaces and growing films. (From Ref. 18)

**A** discharge is essentially a plasma- i.e., a partially ionized gas composed of ions, electrons, and neutral species that is electrically neutral when averaged over all the particles contained within. Moreover, the density of charged particles must be large enough compared with the dimensions of the plasma **so** that significant Coulombic interaction occurs. This interaction enables the charged species to behave in a fluidlike fashion and determines many of the plasma properties. The plasmas used in sputtering are called glow discharges.

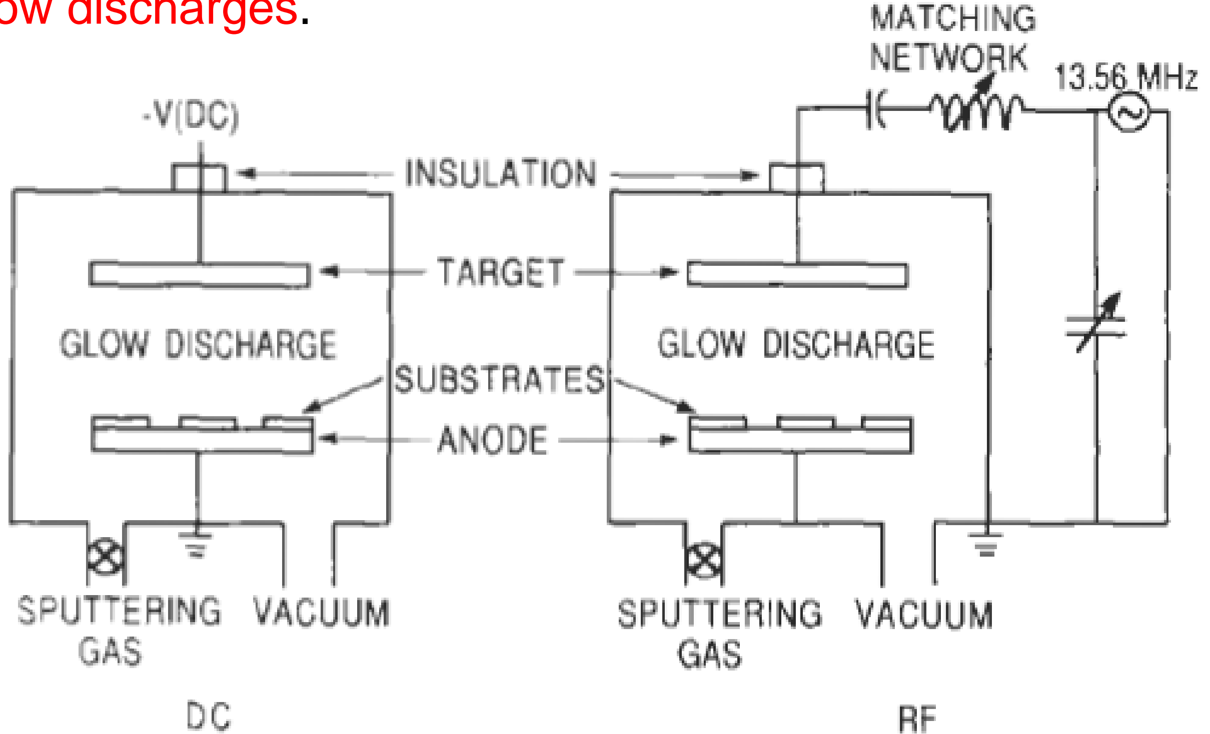


**Figure 3-13.** Schematics of simplified sputtering systems: (a) dc, (b) RF.

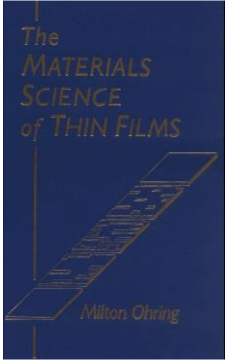

Sputtering sources often employ magnetrons that utilize strong electric and magnetic fields to confine charged plasma particles close to the surface of the sputter target. In a magnetic field electrons follow helical paths around magnetic field lines undergoing more ionizing collisions with gaseous neutrals near the target surface than would otherwise occur. (As the target material is depleted, a "racetrack" erosion profile may appear on the surface of the target.) The sputter gas is typically an inert gas such as argon. The extra argon ions created as a result of these collisions leads to a higher deposition rate. It also means that the plasma can be sustained at a lower pressure. The sputtered atoms are neutrally charged and so are unaffected by the magnetic trap. Charge build-up on insulating targets can be avoided with the use of **RF sputtering** where the sign of the anode-cathode bias is varied at a high rate (commonly 13.56 MHz). RF sputtering works well to produce highly insulating oxide films but with the added expense of RF power supplies and impedance matching networks. Stray magnetic fields leaking from ferromagnetic targets also disturb the sputtering process. Specially designed sputter guns with unusually strong permanent magnets must often be used in compensation.

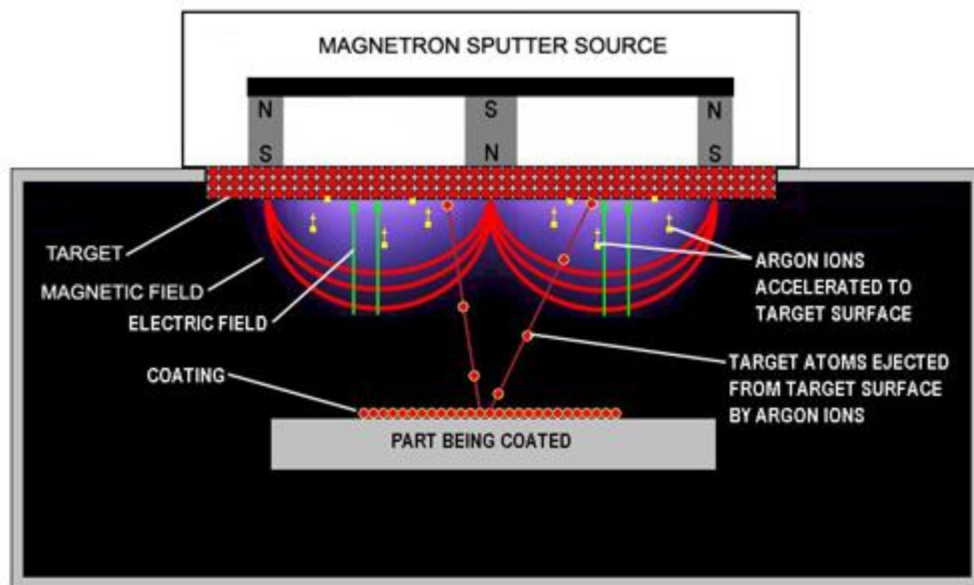

# Pulsed-laser deposition schematics

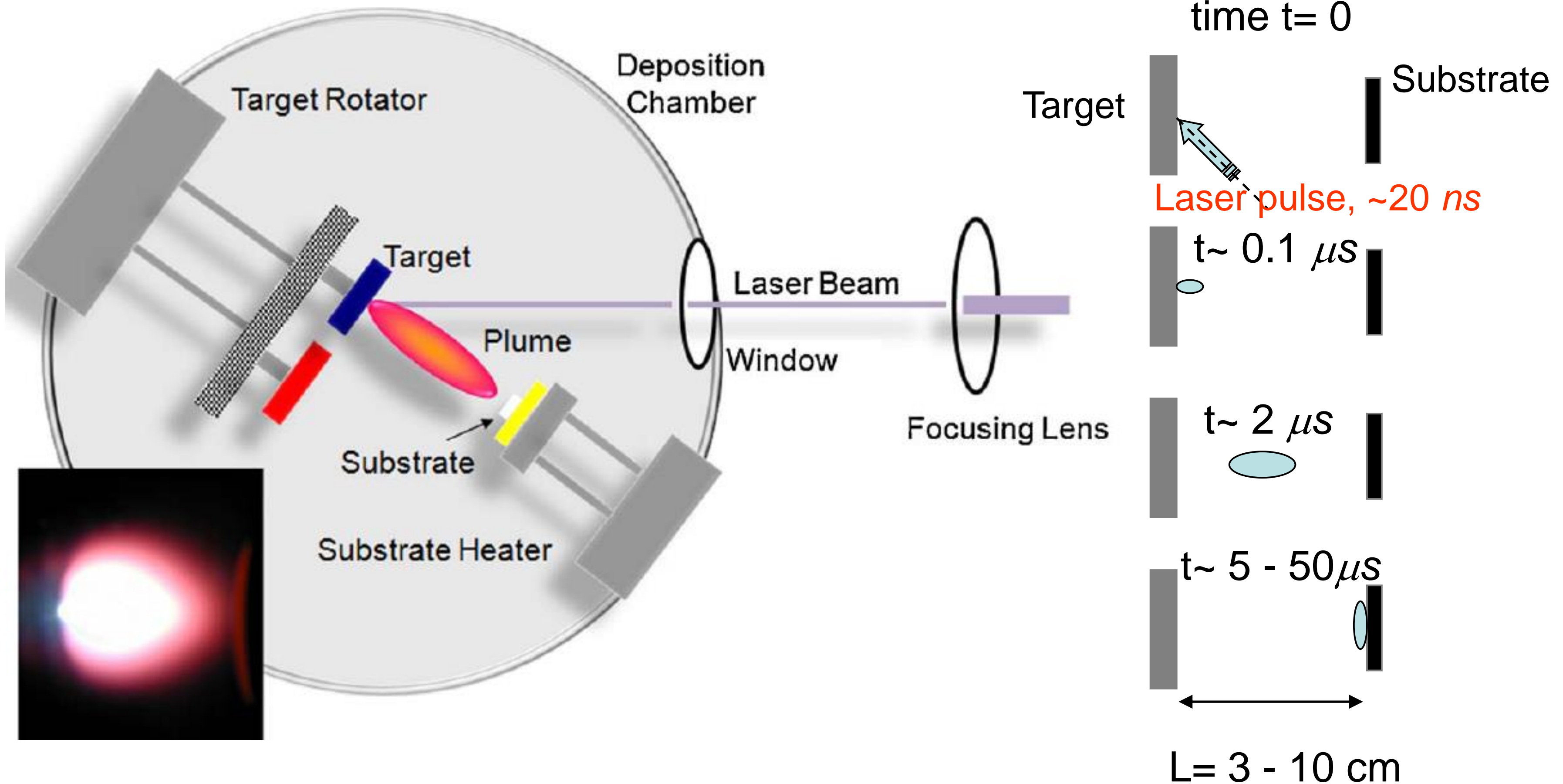

# Pulsed-laser deposition assisted by reflective high energy electron diffraction (RHEED)

Animation of an experiment of growing superconductive films of YBCO on $SrTiO_3$(100) by PLD and monitoring the growth by RHEED

# 1. Laser ablation of the target

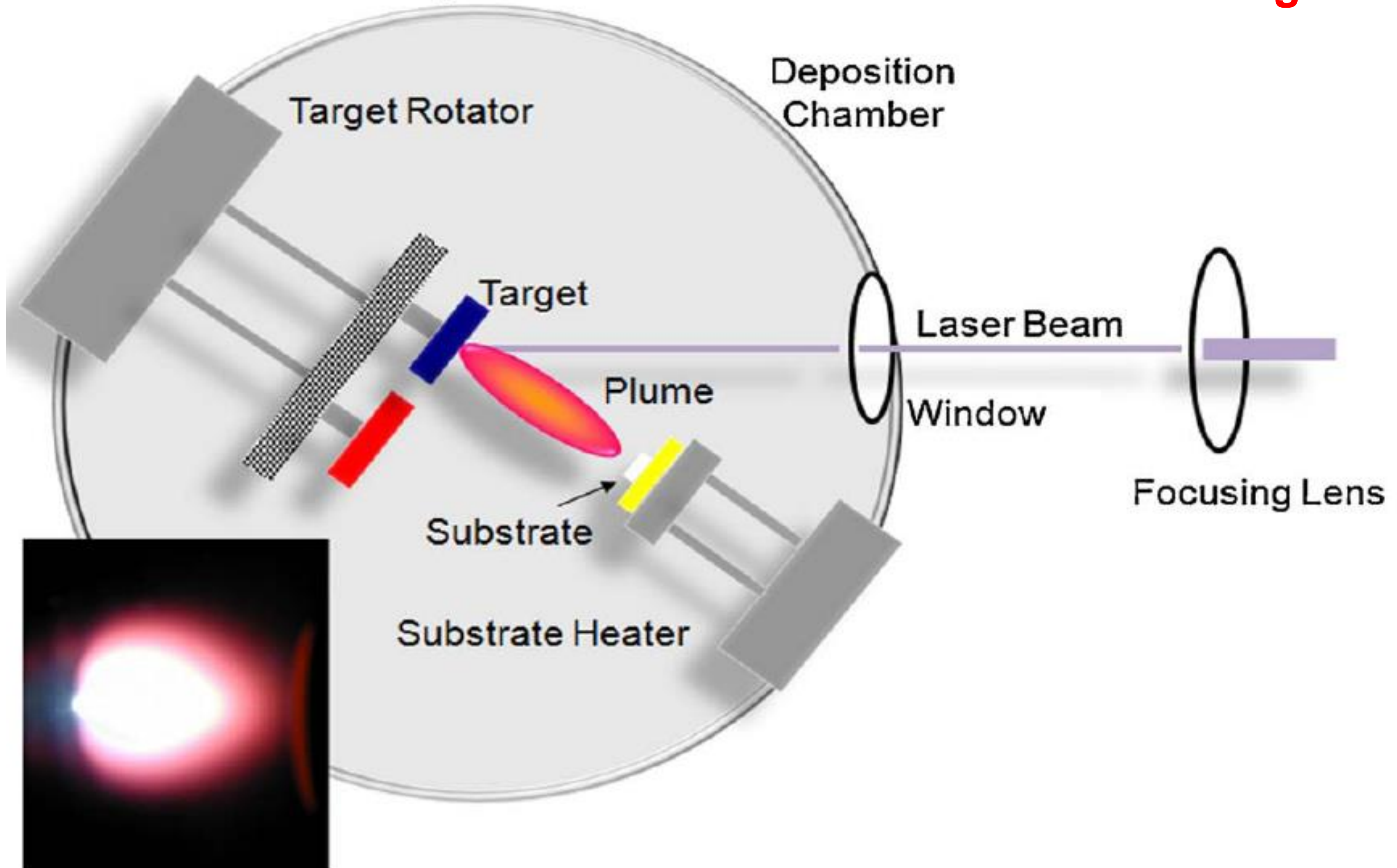

## LASER: Light amplification by stimulated emission of radiation

**Laser light properties:**

✓ ***high spatial coherence*** **→ extreme focusing and directional irradiation of high energy densities**

✓ ***monochromaticity***

✓ ***tunability***

✓ ***controlled pulsed excitation*** **→ high temporal resolution; often makes it possible to overcome competing dissipative mechanisms within the particular system under investigation**

**Types of lasers (based on the active medium):**

**- solid state lasers: ruby laser($Cr^{3+}$:$Al_2O_3$ ,694 nm), $Nd^{3+}$: YAG (1.06 μm, but down to 266 nm by frequency multiplication in nonlinear crystals external to the laser cavity), semiconductor (diode) lasers (IR)**

**- gas lasers: $CO_2$ laser (10.6 μm), HeNe (633 nm) , excimers (157 nm to 351 nm), etc.**

**- dye (liquid solution) lasers (tunable wavelength)**

**The range of wavelengths for fabrication of thin films of complex oxide compounds by PLD lies between 200 nm and 400 nm.**

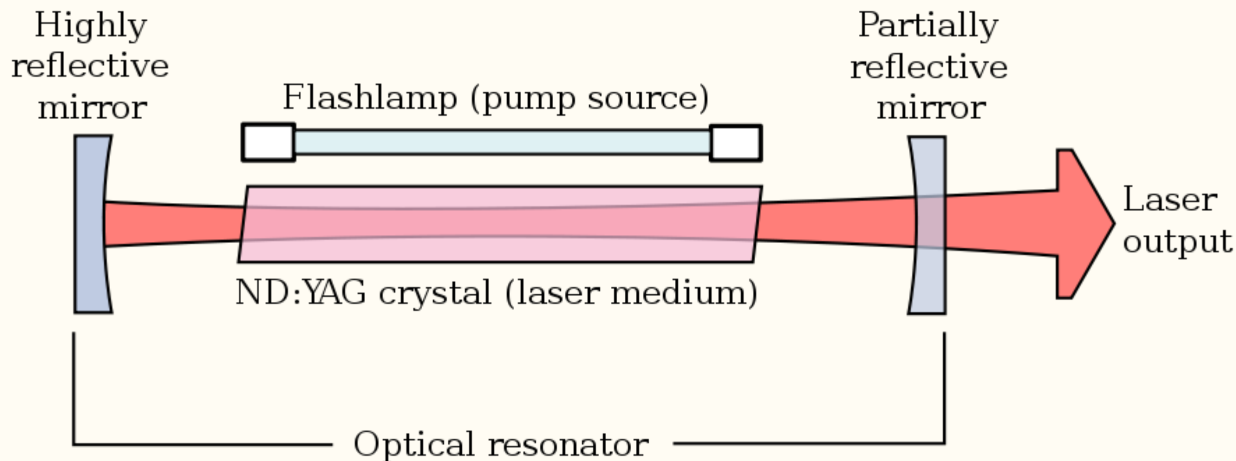


Energy levels of the active medium: $Nd^{3+}$ doped- $Y_3Al_5O_{12}$ (1 at. %, i.e. impurity concentration of $1.36 \times 10^{20}$ $cm^{-3}$)

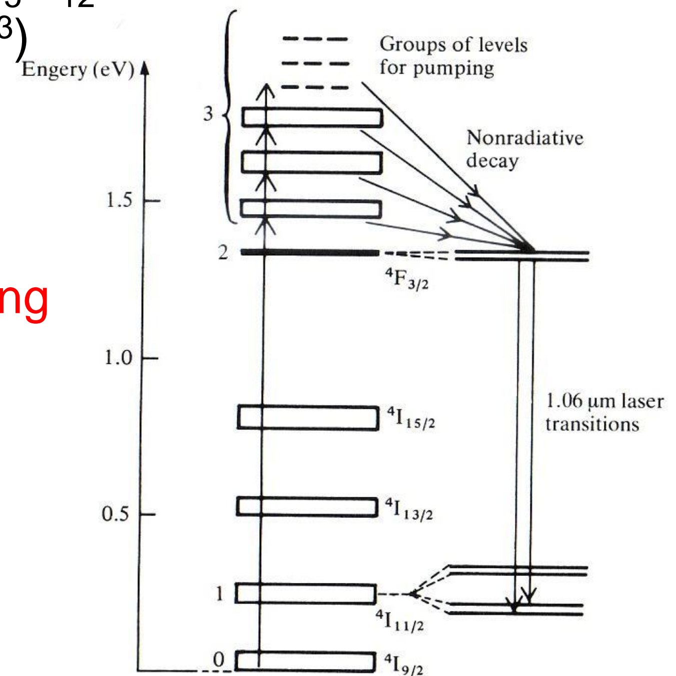


A four levels system
Highest gain lasing at 1064 nm

It can work in continuous wave mode and by Q-switching it can be made to operate in a pulsed regime (typically 10-25 ns duration pulses)

The high-intensity pulses may be efficiently frequency doubled to generate laser light at 532 nm, or higher harmonics at 355 and 266 nm.

# Excimer laser basics

Light output from an excimer laser derives from a molecular gain medium in which lasing action takes place between a bound upper electronic state and a repulsive or weakly bound ground electronic state:

-The excimer molecule (i.e., KrF*) dissociates rapidly, on the order of $10^{-13}$ s as it emits a photon during transition from upper state to ground state.

-High ratio of upper state lifetime to lower state lifetime→ somehow, a perfect laser medium, because the population inversion and therefore high gain are thus easily achieved

The excimer molecules are formed in a gasous mixture, such as Xe, HCl and Ne, in case of XeCl laser.

**Pumping of the laser medium**: avalanche **electric discharge excitation**, creating ionic and electronically excited species that react chemically and produce excimer molecules.

The kinetics and chemical reactions forming the excimer molecules are quite complex, involving many steps.

**Example for KrF** excimer reactions:

(* denotes electronically excited species, X denotes a third body: He, Ne)

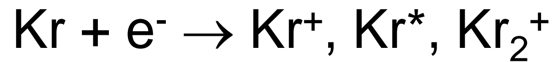

$Kr + e^- \rightarrow Kr^+, Kr^*, Kr_2^+$

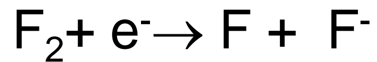

$F_2 + e^- \rightarrow F + F^-$

**$Kr^+ + F^- + X \rightarrow KrF^* + X$** (excimer stabilization by involvement of a third body)

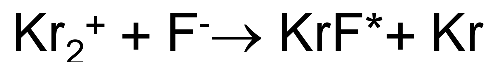

$Kr_2^+ + F^- \rightarrow KrF^* + Kr$

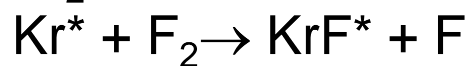

$Kr^* + F_2 \rightarrow KrF^* + F$

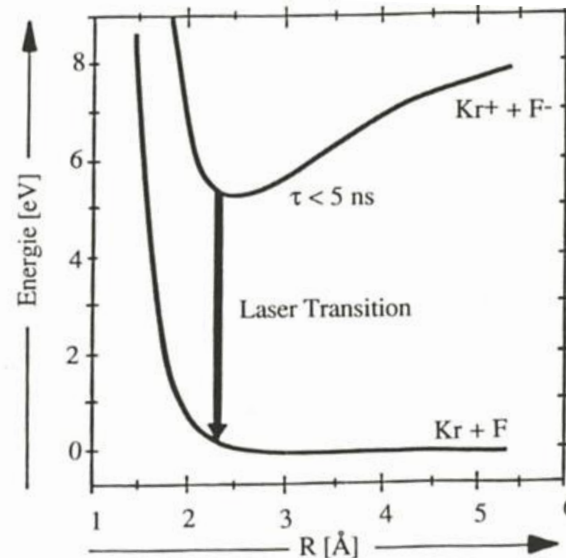


Figure 2.1. Schematic diagram of the electronic potential of the KrF excimer.

From "Pulsed laser deposition of thin Films" by D. B Chrisey & G. K. Huber

Once the excimer molecule is formed, it will decay via spontaneous emission and collisional deactivation→ molecule lifetime of ~2.5 ns

Output energies of several hundred mJ / laser pulse dictate an excimer population density of $10^{15}/cm^3$→***for lasing to occur***, the formation rate of the ionic and excited precursors must be fast enough to produce excimers at a rate of several $10^{23} / cm^3 / s$.

# Excimer lasers

High outputs in excess of 1Joule/pulse may be nowadays achived

Pulse repetition rates of up to several hundred Hertz with energies of 500 mJ/pulse

| Excimer | Wavelegth (nm) |
| --- | --- |
| $F_2$ | 157 (7.9 eV) |
| ArF | 193 |
| KrCl | 222 |
| KrF (highest gain) | 248 (i.e., $h\nu$= 5 eV) |
| XeCl | 308 (4 eV) |
| XeF | 351 |

Lasers - used to pattern/process solid surfaces

- used to fabricate thin films by condensing on a substrate the material that is ablated from a target under the action of laser light (solid or liquid)- *pulsed-laser deposition*.

Laser ablation is a particulary suitable and powerful tool in micropatterning of hard, brittle, and heat sensitive materials or biological materials- “PHOTONS ARE CLEAN”→ surgery tool, see for instance eye surgery LASIK (*laser-assisted in situ keratomileusis*- corneea reshaping )

Pulsed-laser ablation (PLA): material removal caused by short high-intensity laser pulses, taking usually place far from equilibrium; may be based on thermal and non-thermal microscopic mechanisms

# Laser ablation for thin film growth has many advantages:

- The energy (laser) source is outside the vacuum chamber and the photons are "clean".
- Almost any condensed matter can be ablated.
- The pulsed nature of PLD means that film growth rates may be controlled to any desired amount.
- The amount of vaporized source material is localized only to about that area defined by the laser focus.
- Under optimal conditions, the ratios of the elemental components of the bulk and the film are the same, even for very complex compositions.
- The kinetic energies of the ablated species arriving at the substrate lie mainly in a range that promotes surface mobility while avoiding bulk displacements.
- The ability to produce species with electronic states far from chemical equilibrium opens up the potential to produce novel or metastable materials that would be unattainable under thermal conditions.

*Reviews of Modern Physics, Vol. 72, pg. 315-328, 2000*

PLD also has fundamental drawbacks:

- The production of ejecta (particulates) during the ablation process
- Impurities in the target material → transfered to the film
- Crystallographic defects in the film caused by bombardment by high kinetic energy ablation particles
- Inhomogeneous flux and angular energy distribution within the ablation plume

*Reviews of Modern Physics, Vol. 72, pg. 315-328, 2000*

**Schematic of different types of electronic excitations in a (crystalline) solid** (*primary* interactions between light and matter are *always non-thermal,* namely *elementary excitations*):

-straight lines indicate absorption or emission of photons with different energies, $h\nu$; oscillating lines indicate non-radiative processes

- interband transitions for $h\nu \geq E_g$: electron-hole pairs are generated; band-gap excitations are located in the near infrared (NIR) and visible (VIS) for semiconductors and in the ultraviolet (UV) for insulators

- defect-, impurity- and surface states permit sub-bandgap excitations with $h\nu < E_g$

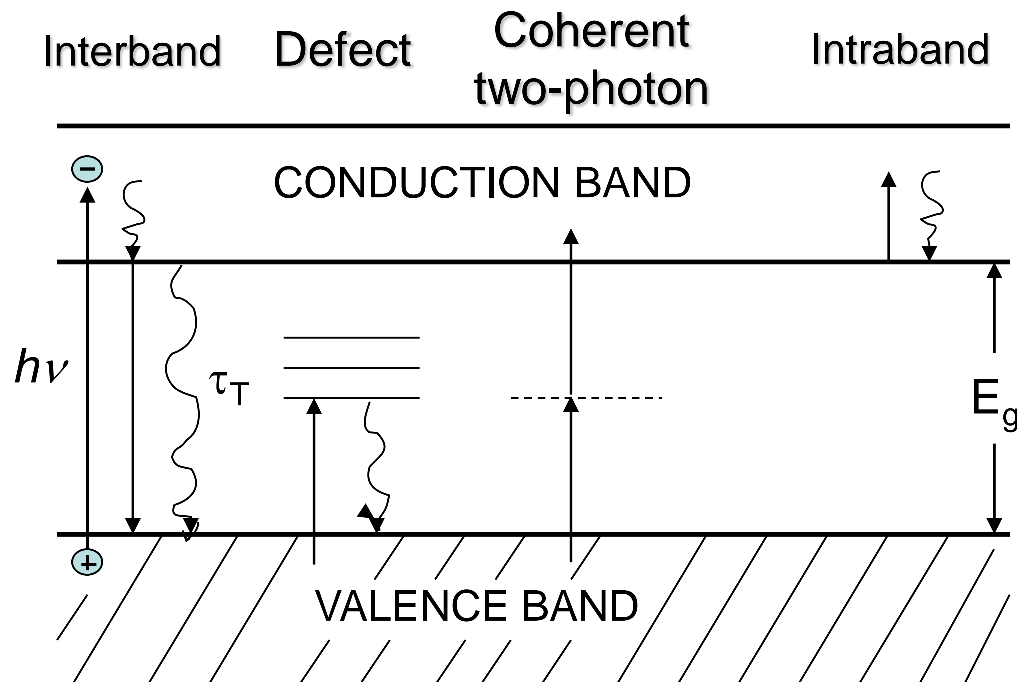

# Laser light-induced thermal processes

Thermalization of the excitation energy described by the relaxation time $\tau_T$.

For a *thermal process*, $\tau_T << \tau_R$, where $\tau_R$ characterizes the initial processing step or the inverse excitation rate (depending which is smaller)→ if $\tau_T << \tau_R$ the detailed excitation mechanisms become irrelevant and the laser can be considered simply as a HEAT SOURCE.

In spite of their thermal character, LASER-DRIVEN thermophysical and thermochemical processes may be quite different from those initiated by a conventional heat source:

- the laser-induced temperature rise can be localized in space and time → $T>10^4$ K can be induced in a small volume that is defined by the focused laser beam
- with short, high-intensity laser pulses, heating rates up to $10^{15}$ K/s can be achieved
- selective excitation of a particular species (e.g., in a gas mixture)
- laser heating may change the optical properties of the medium and thereby introduce non-linearities in the interaction process.

# (Pulsed)-laser ablation (FEEDBACK) mechanisms

*PLAs steps:*
*- optical excitation*
*- energy dissipation*
*- decomposition and removal of material*

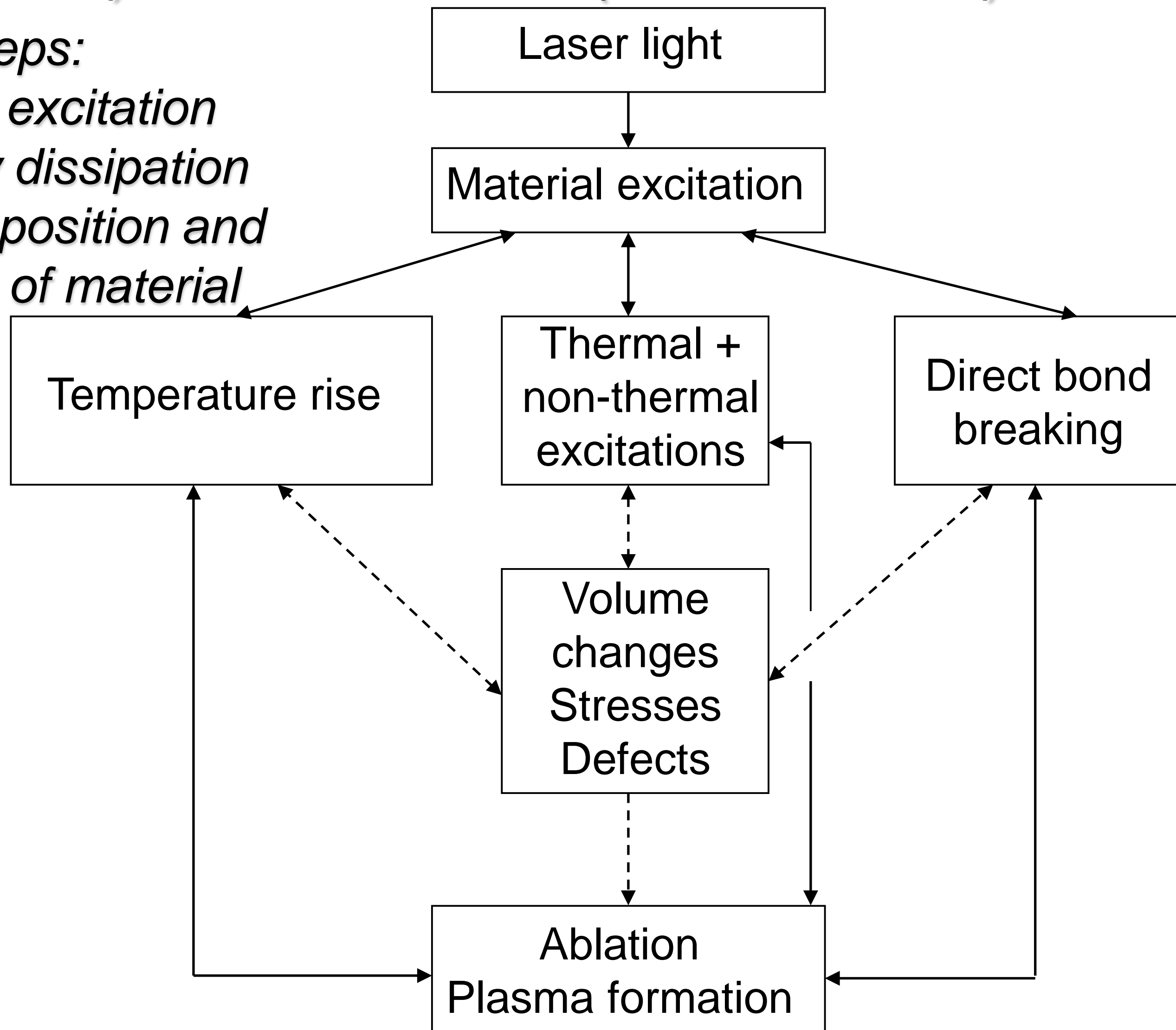


Ablation can be based on thermal activation only (left path), on direct bond breaking (photochemical ablation; right path), or on a combination of both (photophysical ablation; intermediate path).

# Photothermal process: Pulsed-laser ablation

Pulsed-laser ablation:
- removal of material by irradiating a target with laser pulses
- widely supresses the dissipation of the excitation energy beyond the volume that is ablated during the pulse:

this holds if the thickness of the layer ablated per pulse, $\Delta h$, is of the order of the heat penetration depth, $l_T \approx 2(D\tau_l)^{1/2}$, or the optical penetration depth, $l_\alpha = \alpha^{-1}$, depending on which is larger, i.e.

$$\Delta h \approx \max(l_T, l_\alpha) \quad (*)$$

*Nota bene*: because of the fast heating and cooling rates achieved with pulsed lasers, material damage or material segregation in multicomponent systems can be often ignored even in cases where the ablated layer thickness is considerably smaller than the value obtained from (*).

# Laser ablation used for pulsed-laser deposition

$$\Delta h \approx \max(l_T, l_\alpha)$$

is well fulfilled with many materials, such as most oxides, for UV-laser light and *nanosecond*-long laser pulses (excimer lasers).

However, with certain materials, due to their high thermal conductivity, *n*s laser pulses are too long for high-quality and high-resolution surface patterning (metals, many semiconductors, thin films of high $T_C$ superconductors, etc.) The above relation can be fulfilled only with *picosecond*- and *femtosecond*-long laser pulses.

Pulsed-laser ablation (PLA) can be used to fabricate thin films by condensing on a suitable substrate surface the material that is ablated from a (solid or liquid) target.

PLA can be used for the growth of stoichiometric multicomponent thin films if *congruent ablation* regime is achieved, avoiding material segregation, in multicomponent systems.

*Incongruent ablation* (for *insufficient* energy densities of the laser radiation on the target): e.g., due to preferential evaporation of the elements with lower vaporization temperatures and enthalpies, or higher vapor pressures of certain elements → in the laser-irradiated multicomponent target surface-segregation can occur.

## Laser parameters to be optimized* for PLD purposes:

- ✓ Wavelength (few $\mu m$ to 157 *nm)*
- ✓ Pulse duration (tens of *ns* to tens of *fs*)

} Limited choices of laser systems, especially for commercial PLD set-ups

- ✓ Laser energy density on the target (fluence)
- ✓ Laser spot: size and shape
- ✓ Pulse repetition rate (0.1 Hz to few kHz)

} Tunable!

* Proper choice of laser parameters is of great importance, since they determine the type and relative concentrations, the degree of ionization, and the spatial and temporal distributions of species leaving the target surface.

# Threshold laser fluence for (congruent) ablation

Fluence (laser energy density), $\Phi$:

$\Phi$= energy (J) / laser spot area on the target surface ($cm^2$)

- Below threshold or near- threshold ablation regime: for $\Phi<\Phi_{th}$, small quantities of neutral and ionized species become detectable with the most sensitive diagnostics; the amount of the emitted species is highly nonlinear with $\Phi$ and repeated irradiation of the surface at these $\Phi$ does not, however, produce a measureable ablation pit$\rightarrow$ *photodesorption chiefly takes place*

-Threshold for laser ablation, $\Phi_{th}$: for many materials, significant removal rates begin at high temperatures (in the irradiated volume), which, in turn, necessitate high laser energy densities; this fact can be used to define a $\Phi_{th}$ (i.e., the energy density in $J/cm^2$ at which measurable material removal takes place)

- However, a more relevant threshold value for thin film fabrication by PLD is that for congruent (stoichiometric) ablation.

# Threshold laser fluence for stoichiometric ablation

Ex. 1: YBCO stoichiometric ablation

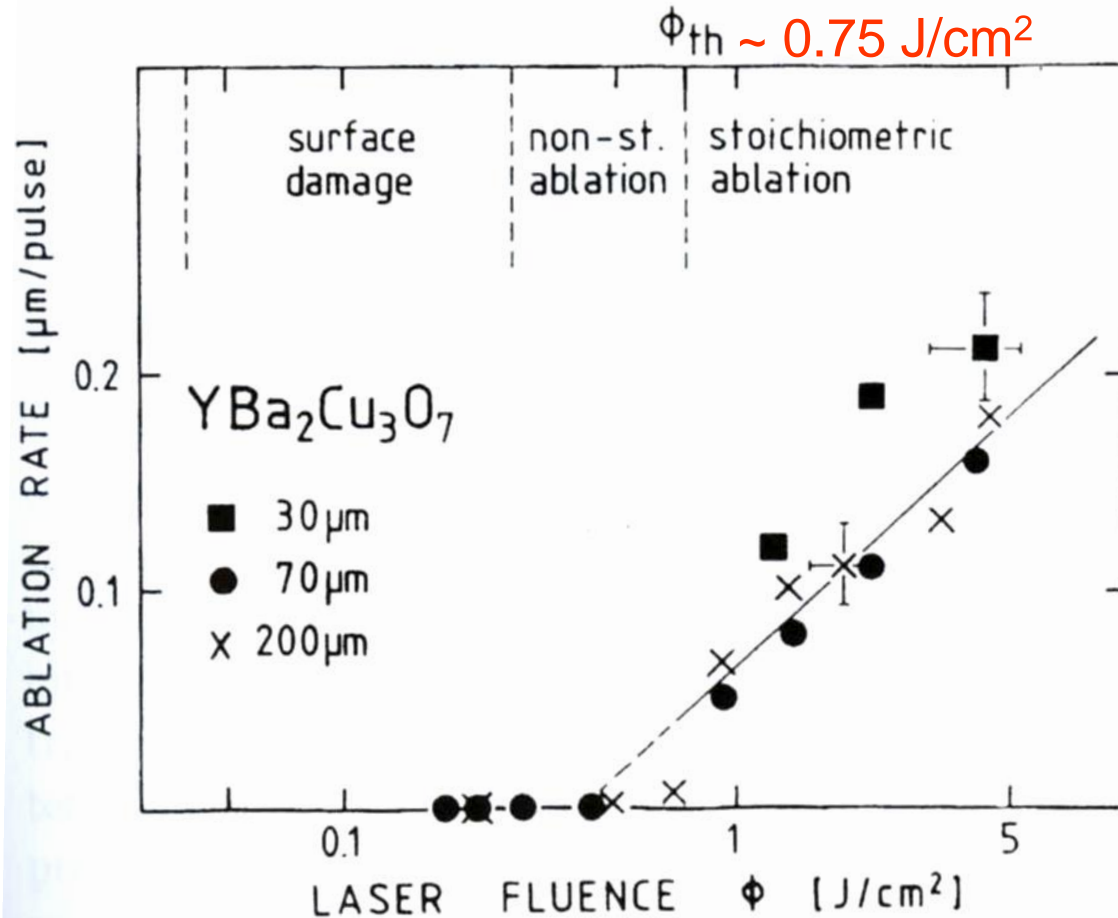


**Fig. 12.4.1.** Surface damage/ablation of $YBa_2Cu_3O_7$ films on (100) MgO substrates as a function of KrF-laser fluence. Different laser-beam spot sizes on the film surface, $2w$, are indicated by different symbols. Film thicknesses were between 0.5 and 1.5 µm [*Heitz* et al. 1990]

*Laser Processing and Chemistry, by Dieter Bäuerle, Springer 2000*

# Ex.2: PLD growth of epitaxial $La_{0.7}Sr_{0.3}MnO_3$ films on $SrTiO_3(100)$ substrates

**T= 850 C**
~$10^{-3}$ mbar$O_2$
L= 5 cm

KrF laser

4 Hz

E= 35 mJ

**Varied the spot size→ varied fluence, but not only…**

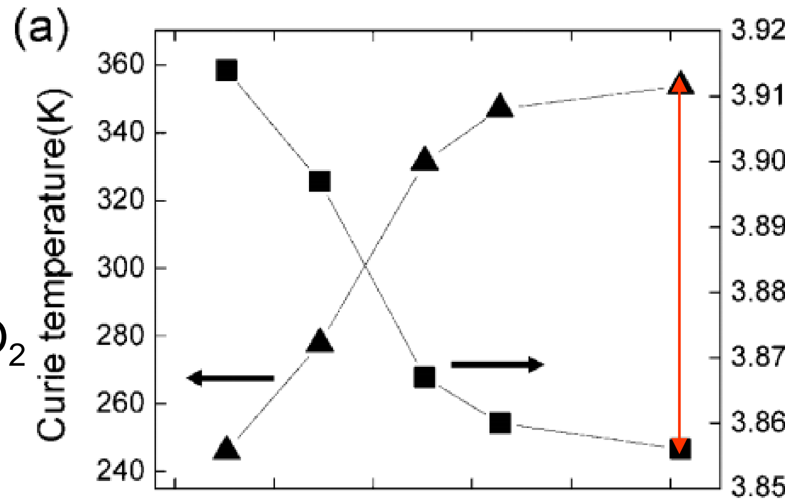


**0.35 J/cm² results in films with best properties**

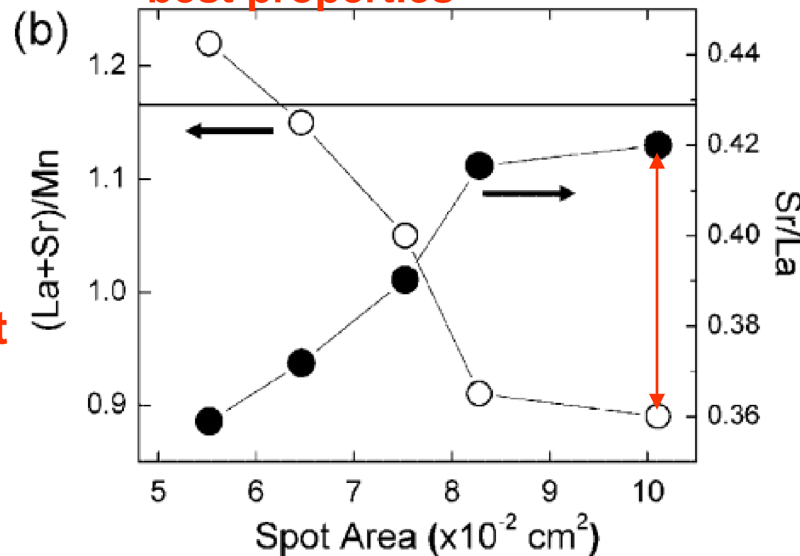


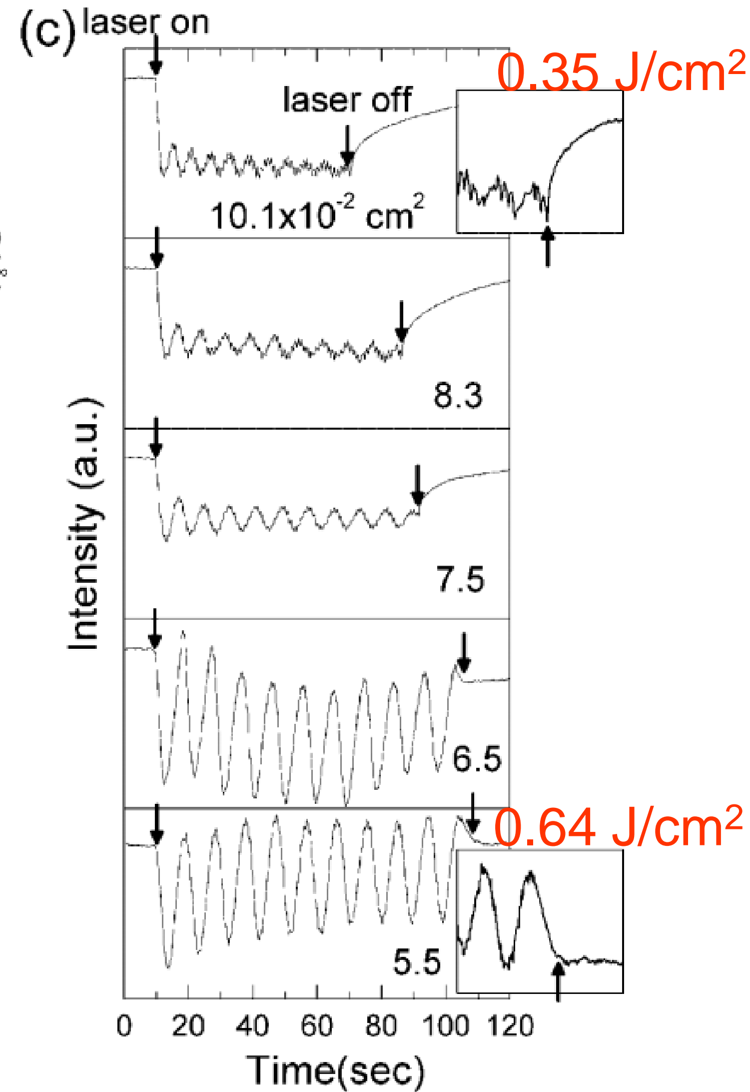


*Adv. Mater.* **2008**, *20*, 2528–2532

**Figure 1.** The effect of laser spot profile on growth. $P_{O_2}$ and $T_g$ during growth were fixed to 1 mTorr and 850 °C, respectively. The total incident laser energy was 35 mJ for all samples studied. a) Variation of $T_c$ and out-of-plane lattice parameters with laser spot area. b) Variation of the cation composition ratios as measured by ICP for thick films grown on GaAs substrates at room temperature. The horizontal line denotes the target Sr/La ratio. c) RHEED intensity oscillations of the specularly reflected beam for growth with different laser spot areas. The arrows indicate the initiation and termination of growth.

APPLIED PHYSICS LETTERS **96**, 032501 (2010)

# Physical properties of $La_{0.7}Ba_{0.3}MnO_{3-\delta}$ complex oxide thin films grown by pulsed laser deposition technique

P. Orgiani,[1,a)] R. Ciancio,[2] A. Galdi,[3] S. Amoruso,[4] and L. Maritato[1]
[1] *CNR-INFM Coherentia and Department of Mathematics and Informatics, University of Salerno, I-84081 Baronissi (SA), Italy*
[2] *CNR-INFM National Laboratory TASC, Basovizza, Trieste I-34012, Italy*
[3] *Department of Physics and CNR-INFM Coherentia, University of Salerno, I-84081 Baronissi (SA), Italy*
[4] *Department of Physics and CNR-INFM Coherentia, University of Napoli Federico II, I-80126 Napoli, Italy*

(Received 11 November 2009; accepted 22 December 2009; published online 22 January 2010)

We report on transport properties of oxide manganite $La_{0.7}Ba_{0.3}MnO_{3-\delta}$ (LBMO) thin films deposited by pulsed laser deposition (PLD) technique. Detailed analysis of heavy-ion stoichiometric composition has been carried out as a function of laser-pulse fluence and ambient oxygen pressure. Depositions using high-fluence (6 J/cm$^2$) and low oxygen pressure ($10^{-2}$ mbar) provide the optimal heavy-ion stoichiometric ratio in the LBMO samples. Deviations from the optimal LBMO stoichiometry are observed when decreasing the laser fluence or increasing the background oxygen pressure. This behavior is interpreted by considering the influence of the experimental deposition conditions on the plume dynamics. All these findings provide clear insights on the PLD-growth of manganites and, more in general, of complex oxide materials. © *2010 American Institute of Physics*. [doi:10.1063/1.3292588]

KrF laser, E= 25 mJ - 200 mJ, L= 4.4- 5.3 cm, **T= 670 °C**, $10^{-2}$ - 1 mbar $O_2$

6.7 J/cm$^2$

JOURNAL OF APPLIED PHYSICS VOLUME 83, NUMBER 6 15 MARCH 1998

# Mechanism of incongruent ablation of $SrTiO_3$

B. Dam,[a] J. H. Rector, J. Johansson, J. Huijbregtse, and D. G. De Groot
*Institute COMPAS and Faculty of Physics and Astronomy, Vrije Universiteit, De Boelelaan 1081, NL-1081 HV Amsterdam, The Netherlands*

(Received 20 October 1997; accepted for publication 26 November 1997)

At low fluences, the [Sr]/[Ti] ratio of laser deposited $SrTiO_3$ films appears to be a function of the laser fluence. The deviation from stoichiometry is remarkably constant in time. From an analysis of both the composition of the film and the irradiated target, we deduce a volume-diffusion-assisted preferential ablation process. At high fluences (above 1.3 J/cm$^2$), stoichiometric $SrTiO_3$ films are obtained. This is not due to a change in ablation mechanism, but follows from the fact that at 1.3 J/cm$^2$ the calculated diffusion length of Sr within the irradiated target, becomes of the order of the ablation rate per shot. © *1998 American Institute of Physics.* [S0021-8979(98)04206-6]

Ceramic stoichiometric $SrTiO_3$ target!

$\Phi_{th}$~ 1.3 J/cm$^2$

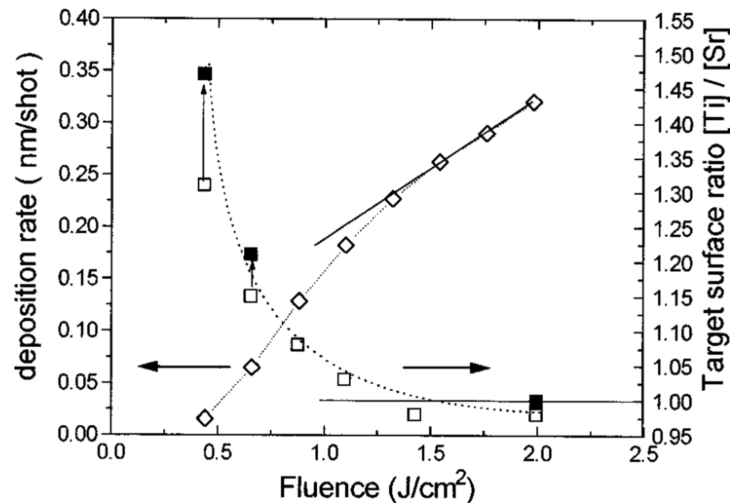


KrF laser (30 *ns* pulse), 5 Hz, L= 3.5 cm

FIG. 1. Deposition rate of $SrTiO_3$ as a function of fluence and the [Ti]/[Sr] composition ratio of the target surface as a function of fluence after 1400 shots (open squares) and after $10^4$ shots (solid squares). The target surface composition is determined from RBS-surface heights of the Sr and Ti signal.

# Target surface modification by cumulative laser irradiation and ejection of *particulates*

From "Pulsed laser deposition of thin films" by D. B Chrisey & G. K. Huber

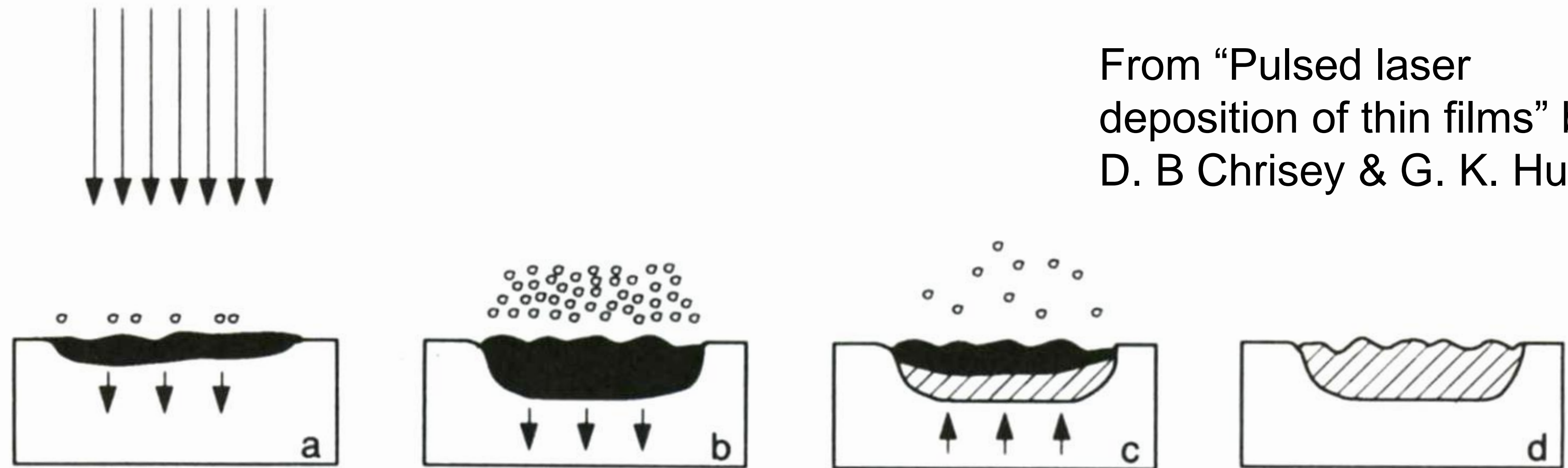


**Figure 4.1.** Schematic of the basic thermal cycle induced by a laser pulse. (*a*) Laser pulse is absorbed, melting and vaporization begin (shaded area indicates melted material, arrows indicate motion of the solid–liquid interface). (*b*) Melt front propagates into the solid, accompanied by vaporization. (*c*) Melt front recedes (cross-hatched area indicates resolidified material). (*d*) Solidification complete, frozen capillary waves alter surface topography. The next laser pulse will interact with some or all of the resolidified material.

# Irradiation at PLD fluence levels: cone formation

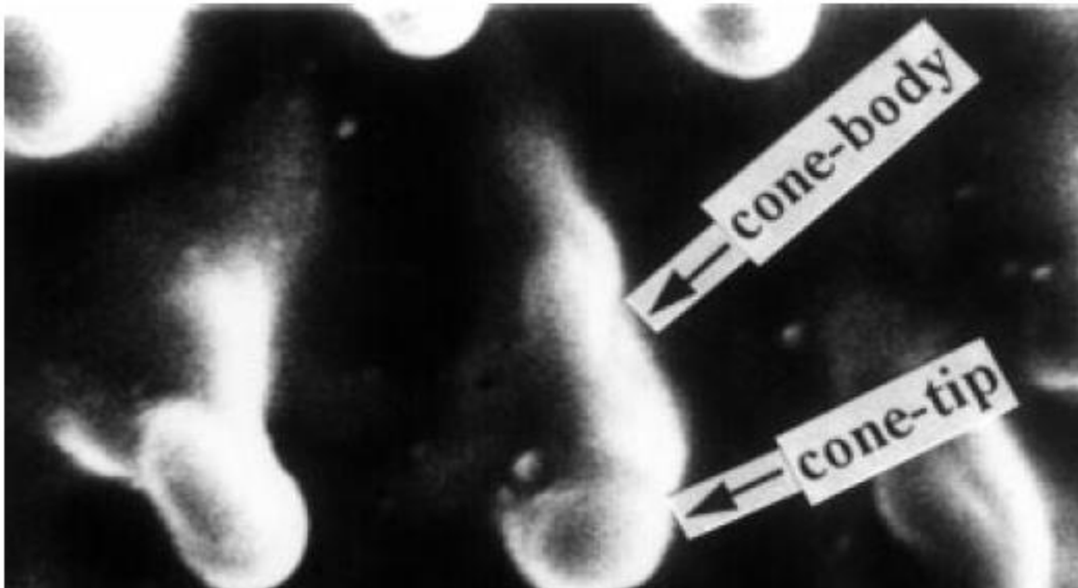


$PbZr_{0.53}Ti_{0.47}O_3$ (PZT) ceramic target

Pb deficiency in the cone tip!

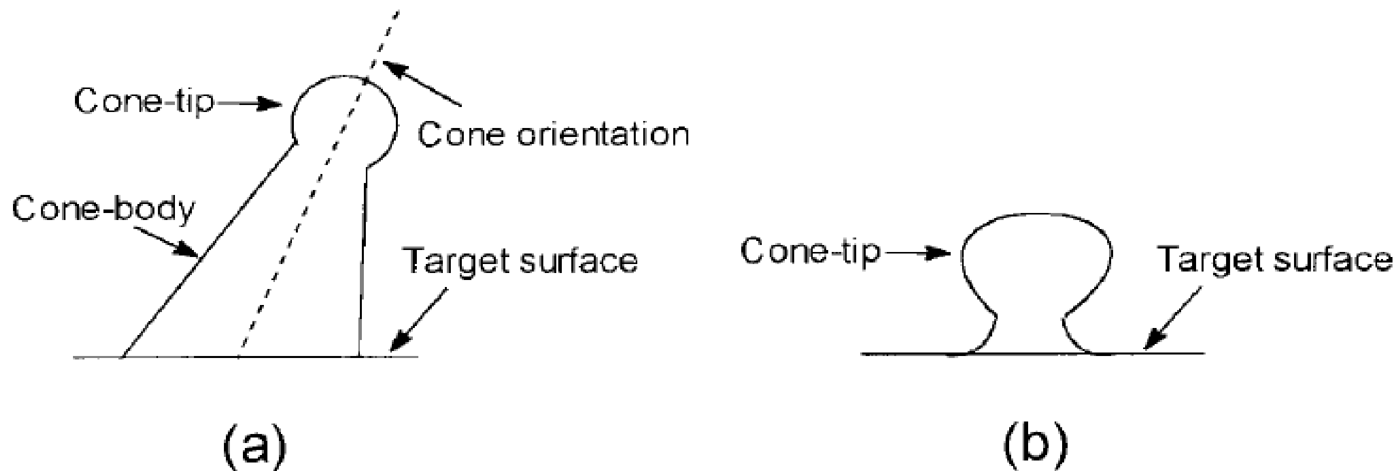


**Fig. 4a,b.** Schematic drawing of two kinds of cone structures. **a** Well-defined cone tip and cone body. **b** Cone tip. The former is basically directed to the laser beam but with deviation to some extent, and the later is almost perpendicular to the local target surface

23–S525 (1999)

di-

# Cone formation on ablated YBCO targets

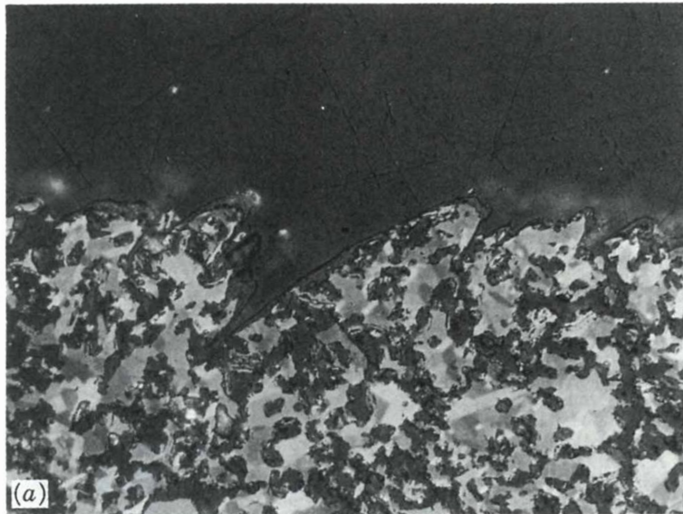

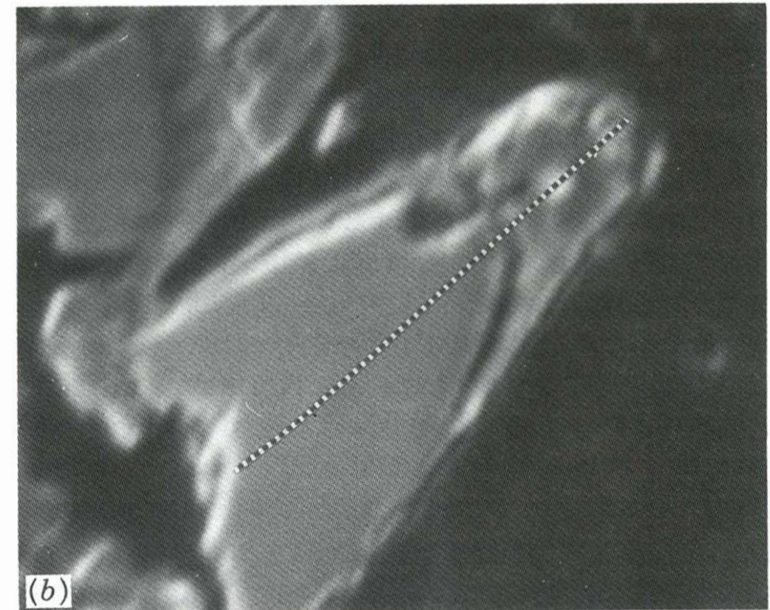

**Figure 4.7.** (*a*) Optical micrograph of a sectioned and polished YBCO target with cones that have formed after 1000 shots/site at a 308-nm fluence of $2\,J/cm^2$. The laser was incident at 45° from the upper right. A modified shell, visible on the surface, surrounds undisturbed polycrystalline target material inside the cones. The field of view is 200 $\mu$m. (*b*) SEM of a different cone on the same target. (*c*) Electron microprobe scan along the dashed path in Figure 4.7*b*. The cone interior has the 1-2-3 composition characteristic of the original target; as the scan enters the tip region, an enrichment of yttrium is measured, along with a corresponding decrease in copper and barium concentrations.

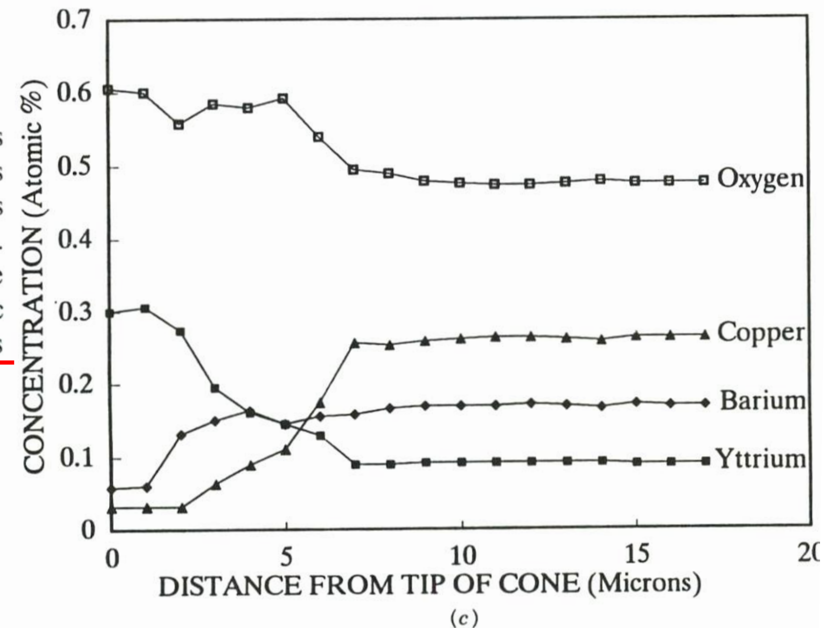


*Pulsed laser deposition of thin films*
by D. B Chrisey & G. K. Huber

# Effects of surface modification on pulsed-laser deposition:

1. On film composition: surprisingly, target surface modification has benign effects, target preconditioning (preablation) is however necessary!
2. On film deposition rate: quite affected!

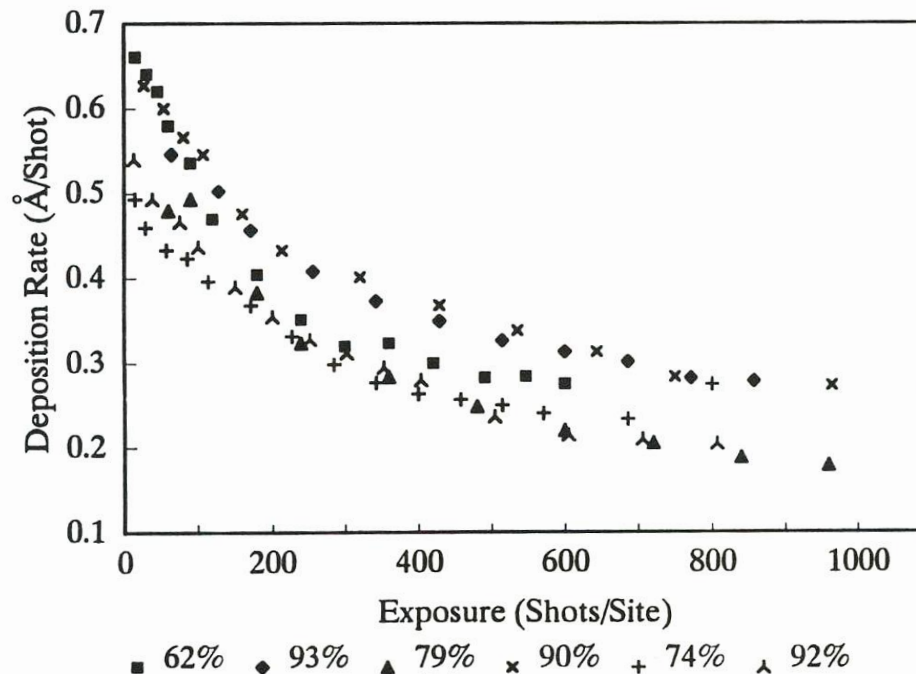


**Figure 4.9.** A set of exposure curves for six different YBCO targets illustrating that rate decay is independent of target microstructure. The legend refers to target density, expressed as a percentage of theoretical maximum.

*Rapid communication* Appl. Phys. A 68, 363–367 (1999)

# Uniform target ablation in pulsed-laser deposition

N. Arnold, D. Bäuerle

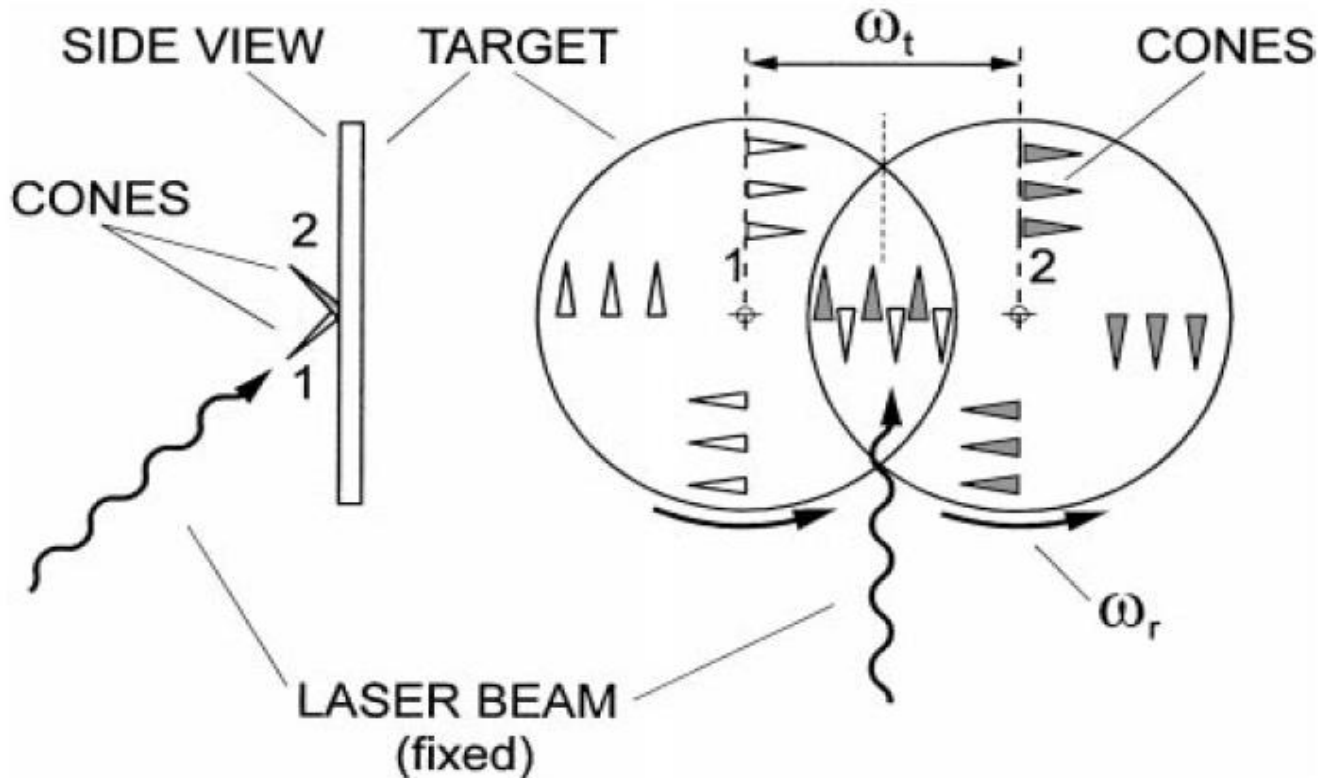


**Fig. 1.** Surface structures which align with the incident laser beam, e.g. columnar structures (cones), can be suppressed by simultaneous rotation and translation of the substrate with frequencies $\omega_r$ and $\omega_t$, respectively. If the translation is symmetric with respect to the incident laser beam, each target site is ablated from opposing incident angles

# One of the solutions against droplets/particulates in PLD films:

See more in *Laser Processing and Chemistry, by Dieter Bäuerle, Springer 2000*

*P.R. Willmott / Progress in Surface Science 76 (2004) 163–217*

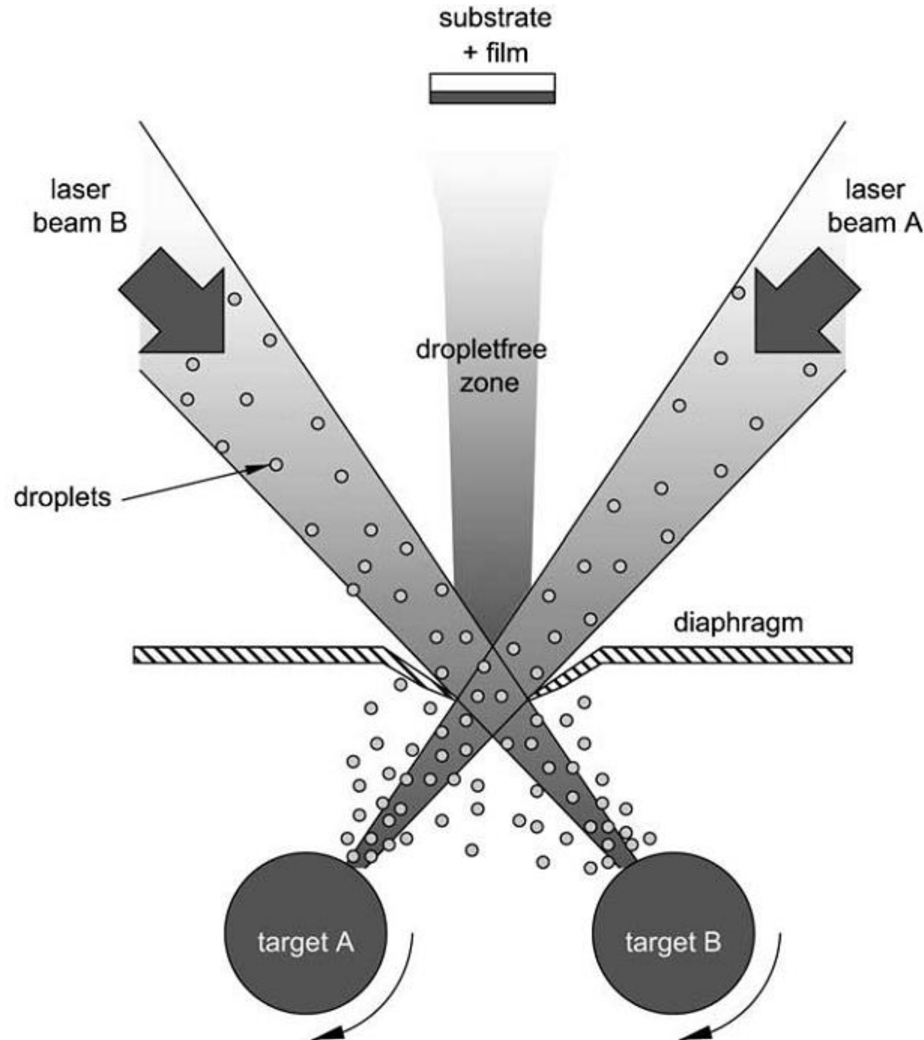

## 2. Plasma expansion and propagation

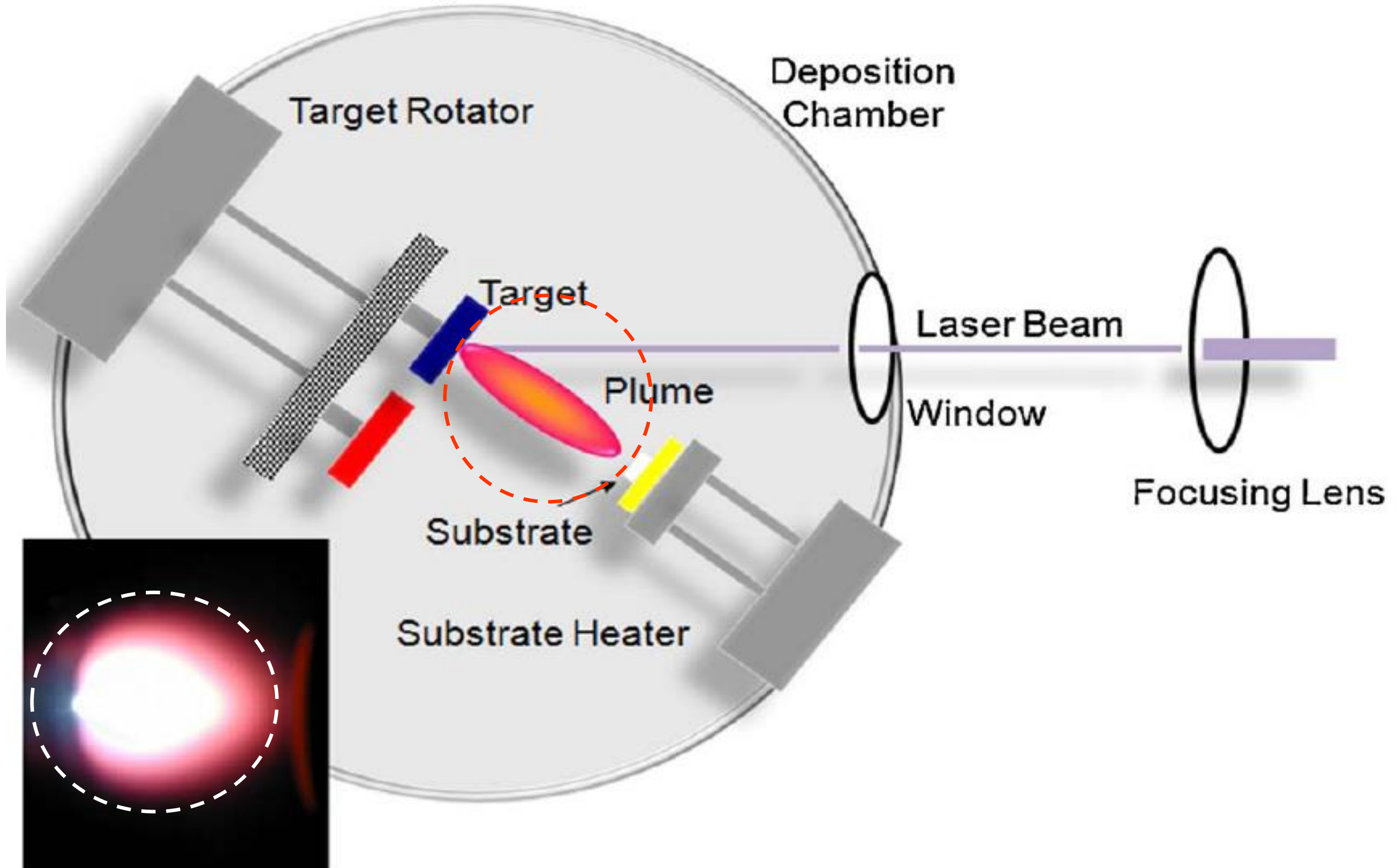

Based on the nature of interaction of the laser beam with the target and the evaporated material, the pulsed-laser ablation process can be classified into three separate regimes:

- interaction of the laser beam with the bulk target,
- plasma formation, heating, and initial three-dimensional isothermal expansion, and then adiabatic expansion and
- deposition of thin films.

The three-dimensional expansion of this plasma gives rise to the characteristic spatial thickness and compositional variations observed in laser-deposited thin films of multicomponent systems.
The forward-directed nature of the laser evaporation process has been found to result from anisotropic expansion velocities of the atomic species which are controlled by the dimensions of the expanding plasma.

# Interaction of the laser beam with the evaporated material from the target material

Absorption coefficient of the laser-induced plasma, $\alpha_P$:

$$\alpha_p = 3.69 \times 10^8 (Z^3 n_i^2 / T^{0.5} \nu^3)[1 - \exp(-h\nu/kT)]$$

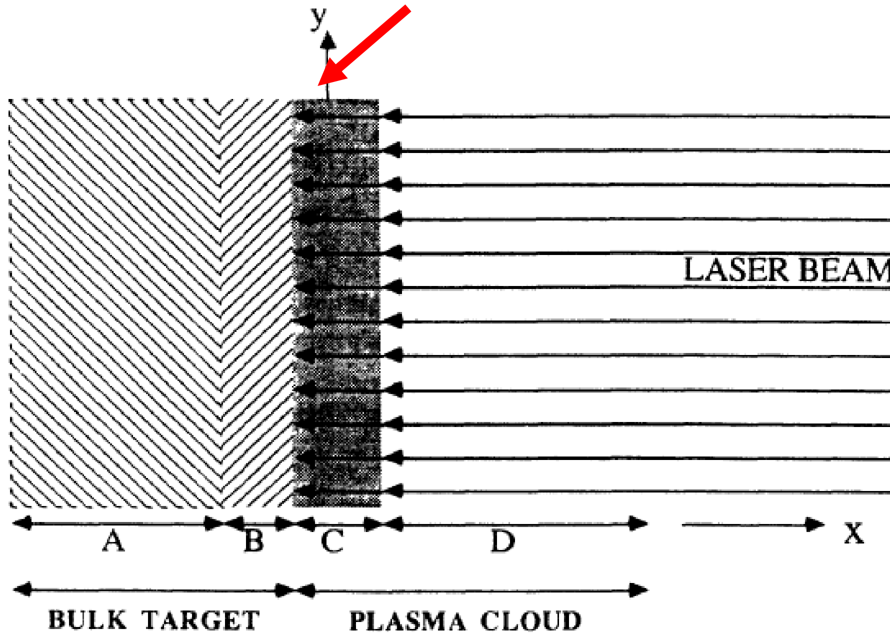


FIG. 1. Schematic diagram showing the different phases present during laser irradiation of a target: (*A*) unaffected target, (*B*) evaporated target material, (*C*) dense plasma absorbing laser radiation, and (*D*) expanding plasma outer edge transparent to the laser beam.

*R. K. Singh and J. Narayan, Phys. Rev. B 41, 8843, 1990*

Z- avearge charge of the plasma components

$n_i$- ion density

$\nu$- frequency of the laser light

The primary absorption mechanism for a plasma is the electtron-ion collisons; the absorption occurs by an inverse bremsstrahlung process, which involves the absorption of a photon by a free electron.

The laser energy is highly absorbed if $\alpha_P X$ is large, where $X$ is the dimension perpendicular to the target of the expanding plasma.

# Influence of laser spot size and shape

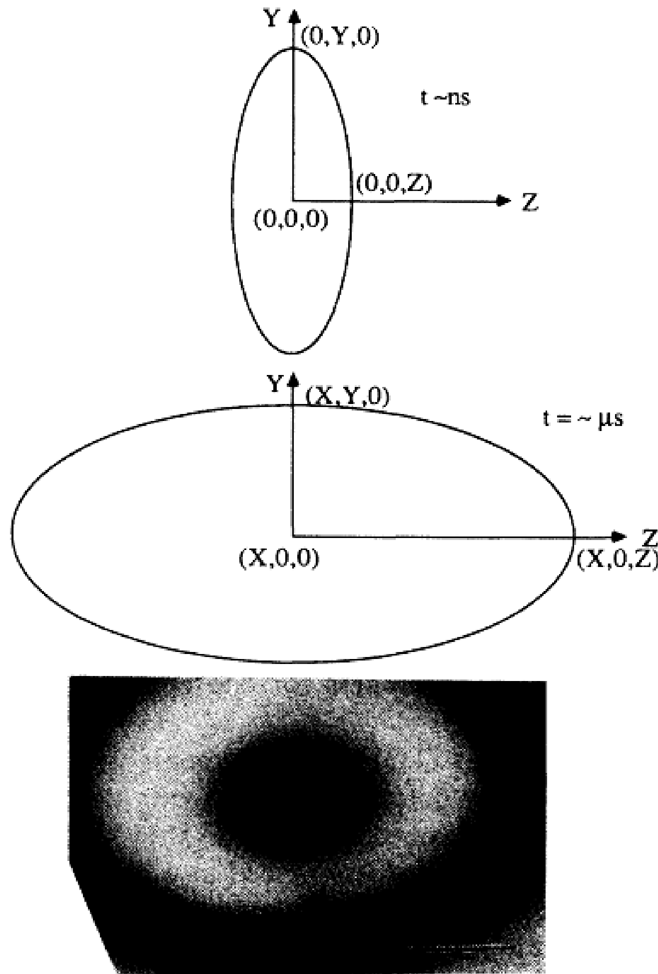


FIG. 3. (a) Schematic diagram showing the initial elliptical plasma shape after termination of the laser pulse, and (b) the final shape of the plasma before it strikes the substrate. The major axis of both of these diagrams are perpendicular to each other. (c) Actual shape of the deposit from a 1:2:3 target on Si showing equithickness contours.

Assuming adiabatic plasma expansion and no spatial temperature gradients after the laser pulse ends:

$$T[X(t)Y(t)Z(t)]^{\gamma-1} = \text{const}$$

$\gamma$ - adiabatic exponent of the vapor

$$X(t)\left[\frac{d^2X}{dt^2}\right] = Y(t)\left[\frac{d^2Y}{dt^2}\right] = Z(t)\left[\frac{d^2Z}{dt^2}\right] = \frac{kT_0}{M}\left[\frac{X_0Y_0Z_0}{X(t)Y(t)Z(t)}\right]^{\gamma-1} \quad t > \tau$$

Where $X_0$, $Y_0$, $Z_0$ are the initial dimensions of the plasma at $t = \tau$ (laser pulse duration)

*R. K. Singh and J. Narayan, Phys. Rev. B 41, 8843, 1990*

PHYSICAL REVIEW B VOLUME 48, NUMBER 16 15 OCTOBER 1993-II

# Gas dynamics and film profiles in pulsed-laser deposition of materials

S. I. Anisimov
*L. D. Landau Theoretical Physics Institute, Russian Academy of Sciences, 142432 Chernogolovka, Moscow Region, Russia*

D. Bäuerle
*Angewandte Physik, Johannes-Kepler-Universität Linz, A-4040 Linz, Austria*

B. S. Luk'yanchuk
*General Physics Institute, Russian Academy of Sciences, 117942 Moscow, Russia*
(Received 25 March 1993)

Film-thickness profiles obtained in pulsed-laser deposition are calculated by using the well-known solution of the gas-dynamic equations which describes the expansion of the plasma plume in vacuum. The time for plasma formation is supposed to be short compared with the time of expansion. The film profile depends on the initial dimensions of the plume and on the adiabatic exponent of the vapor.

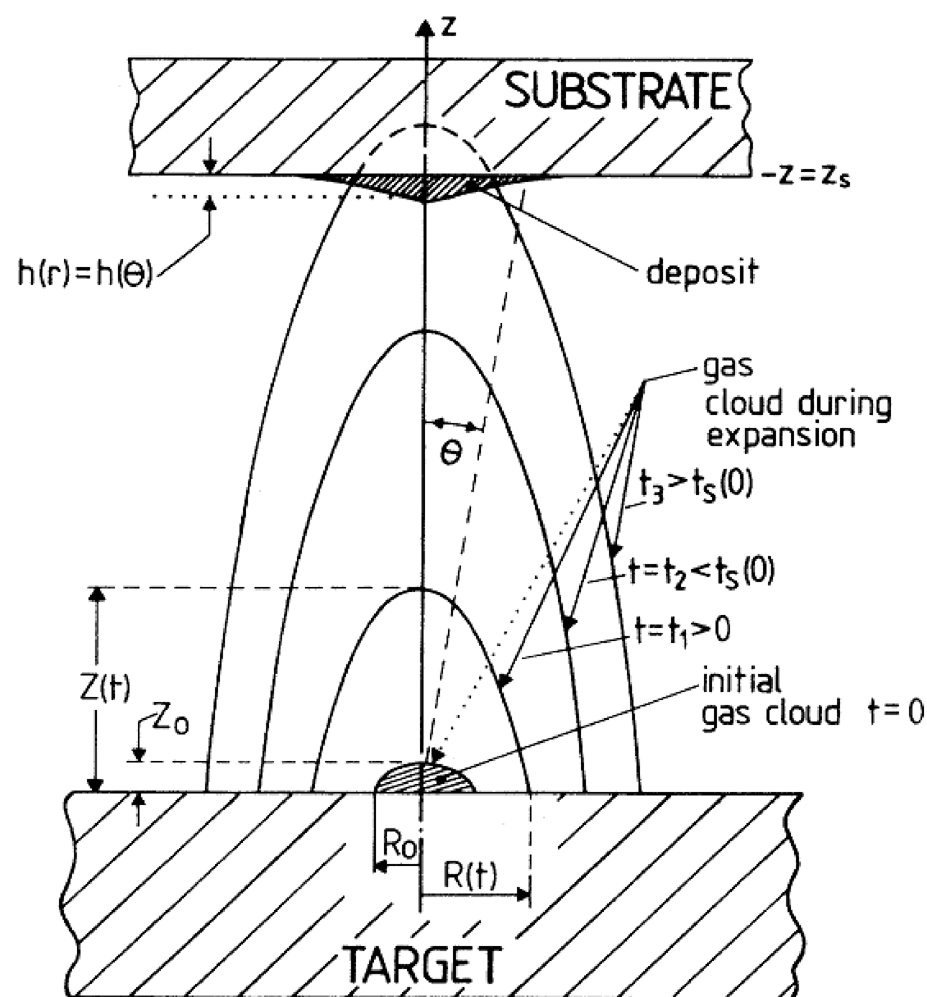


FIG. 1. Schematic for the gas cloud expansion and the deposition of a thin film. The initial gas cloud was created at $t=0$ (after the end of the laser pulse) near the target surface. The gas cloud remains elliptical during its expansion for $t>0$ (see text). The ablated material which reaches the substrate at $z=z_s$ condenses and thereby forms the thin film. The profile of the film is $h(r,t)=h(\theta,t)$, where $r$ is the radial coordinate and $\theta$ the radial angle, $\theta=\arctan r/z_s$.

S. I. ANISIMOV, D. BÄUERLE, AND B. S. LUK'YANCHUK

Appl. Phys. Lett. 56 (6), 5 February 1990

# Effects of beam parameters on excimer laser deposition of $YBa_2Cu_3O_{7-\delta}$

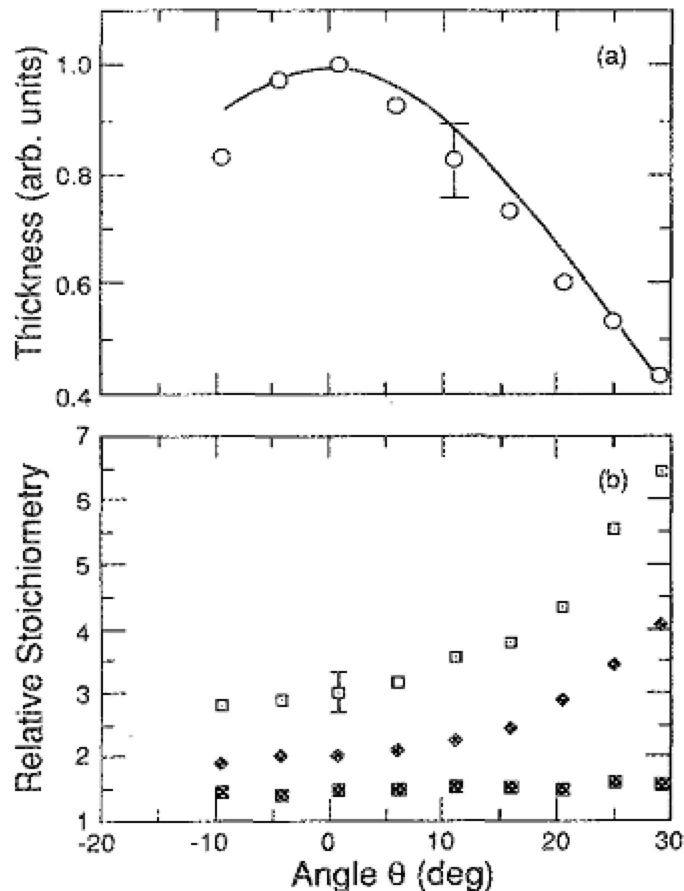


FIG. 2. Film thickness and stoichiometry parallel to the long axis of the focused laser beam, as monitored by RBS, for a film deposited at 5 J/cm², aspect ratio $A_r = 5$, and an oxygen pressure of 0.1 Torr. Part (a) displays thickness and (b) stoichiometry, both as a function of angle. Open squares for the Cu/Y ratio, closed diamonds for Ba/Y, and closed squares for Cu/Ba. The error bars are representative of all data, and follow from a complete error propagation analysis.

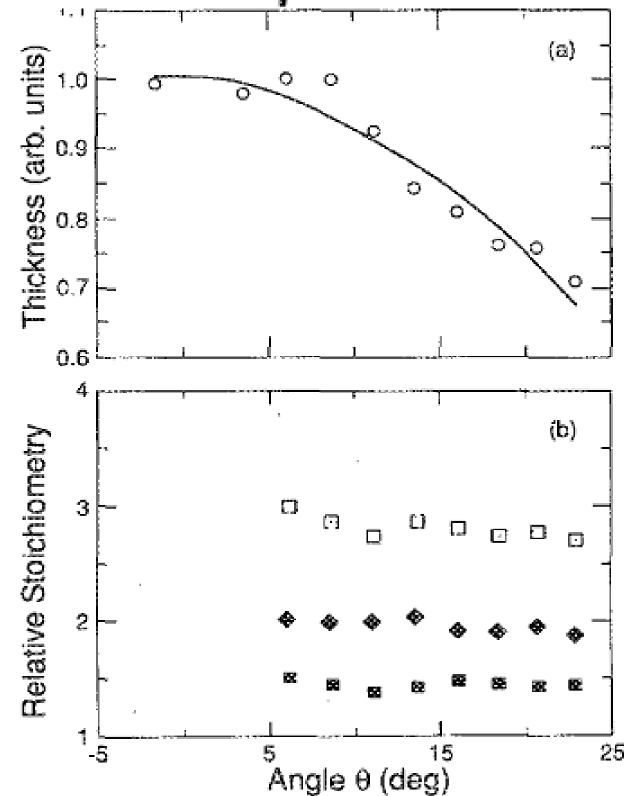


FIG. 3. Similar to Fig. 2, except that data are displayed for the direction perpendicular to the long axis of the focused beam. Part (a) displays thickness as a function of angle, while (b) shows the stoichiometry in this dimension.

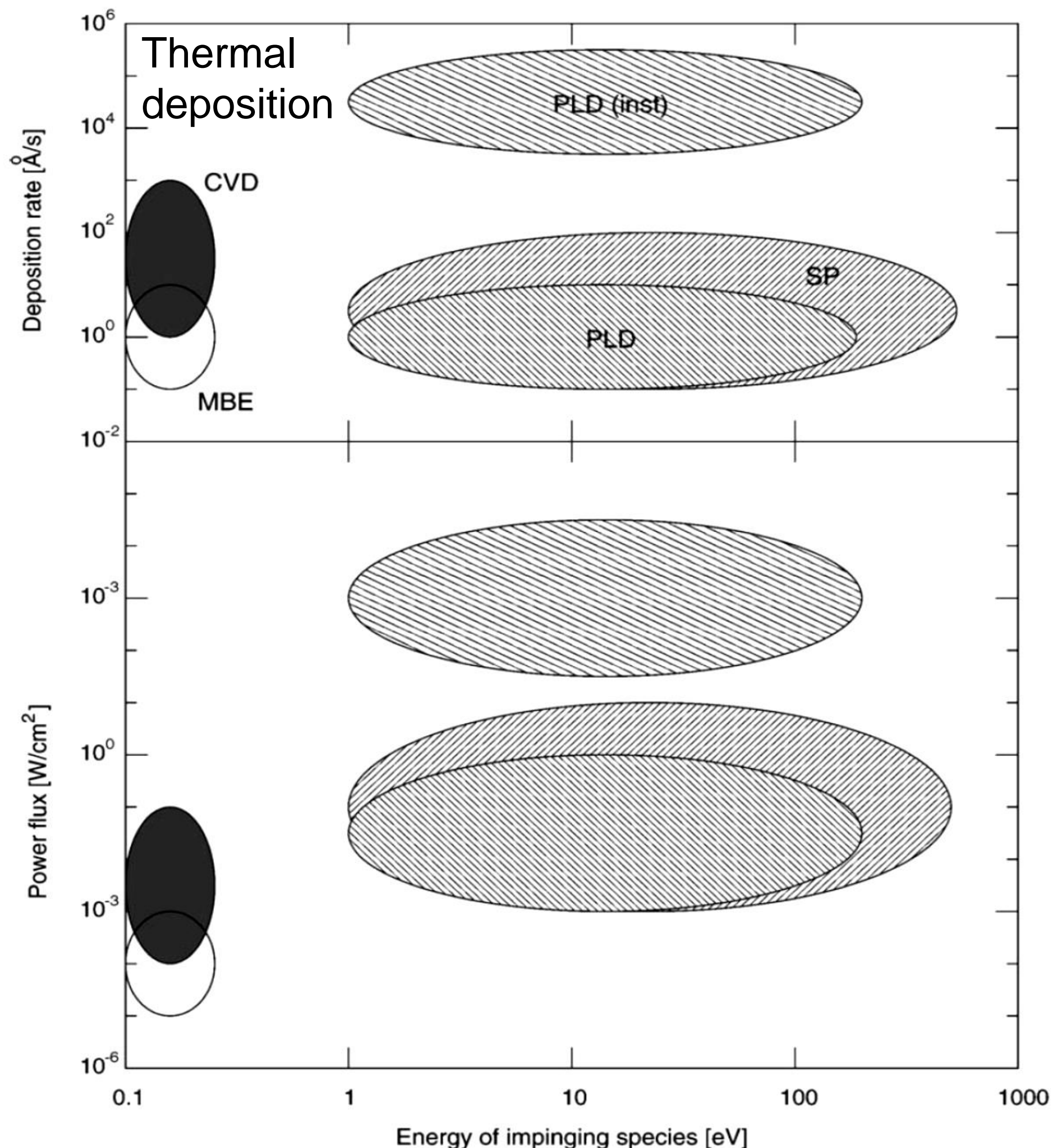


Fig. 8. The power flux and deposition rate versus the energy of the impinging species for CVD, MBE, sputter deposition, and PLD (average and instantaneous). Adapted from Ref. [33] by permission of John Wiley & Sons, Inc. Copyright (1994, G.K. Hubler).

Typical conditions for epitaxial film growth by PLD (at ambient pressures as high as 200 mTorr) involve a large number of gas phase collisions of the ablated material between the target and the substrate, reducing both the ion fraction and the kinetic energy of the evaporated material → near-thermal energies of the species arriving at the substrate!

## What is unique about the way in which film growth proceeds when the vapor-generation and vapor-transport mechanisms involve *pulsed-laser ablation*?

- HIGHLY NON-EQUILIBRIUM and thus NONTHERMAL nature of pulsed-laser deposition makes it one of only a few techniques that is able to transfer chemically complex material *congruently* from the bulk target to the growing thin film.

- PULSED nature of the FLUX of ATOMS (of the order of $10^{20}$ atoms $cm^{-2}$ $s^{-2}$) and associated SUPERSATURATION of the vapor above the substrate surface promote the initial dense nucleation of small two-dimensional islands, which help promote two-dimensional film growth.

- Nonthermal interaction of ENERGETIC incident atoms (up to 1000 eV) with the surface (occurs on the *picosecond* time scale) and it is followed by thermal diffusion processes on the time scale of seconds.

*Pulsed laser vaporization and deposition, P. R. Willmott and J. R. Huber, Reviews of Modern Physics, Vol. 72, pg. 315-328, 2000*

# BIBLIOGRAPHY


- *Laser Processing and Chemistry, by Dieter Bäuerle, Springer 2000*
- *Pulsed laser deposition of thin films, ed. By Douglas. B. Chrisey and Graham K. Huber, New York, Wiley 1994*
- *Pulsed laser deposition of thin films: application-led growth of functional materials, ed. By Robert Eason, Wiley-Interscience 2007*
- *Pulsed laser vaporization and deposition, P. R. Willmott and J. R. Huber, Reviews of Modern Physics, Vol. 72, pg. 315-328, 2000*